UNIVERSITY OF GOTHENBURG

DEPARTMENT OF EARTH SCIENCES

Determining degree and spatial variation of tetrachloroethylene degradation in groundwater using compound-specific isotope analysis (CSIA) of carbon at the Blekingegatan site in Helsingborg

Moa Viklund

Supervisor: Philipp Wanner, Department of Earth Sciences
Examiner: Mark Peternell, Department of Earth Sciences

Degree project for Bachelor of Science with a major in Earth Sciences
2023, 180 HEC
First cycle
B1275

Abstract

Chlorinated solvents have been used as cleaning detergents in dry cleaners throughout the 20th century which has led to the spread of chlorinated solvents in the environment. Blekingegatan, Helsingborg, is a residential area where dry cleaning activities from 1930 to 1979 has led to vast emissions of the chlorinated solvent tetrachloroethylene (PCE). This has resulted in the formation of a groundwater contamination plume in the southwest direction from the source. The aim of this investigation is to establish if degradation of PCE is taking place in the contamination plume and if the magnitude of the degradation is enough to use monitored natural attenuation (MNA) as the remedial method. By measuring concentrations and conducting compound-specific isotope analysis (CSIA) in the sampled groundwater, the spatial variability of concentration- and isotope data could be determined. Results showed high concentrations of contaminants primarily in the source zone while values of the CSIA suggested that degradation is limited and mainly occurs downstream from the source. Furthermore, the values of the degradation product TCE indicated that TCE may be a primary contaminant as well. By constructing a Rayleigh plot it was concluded that dilution rather than degradation is the main contributor to the decrease of the contaminant concentration. Due to these results the extent of degradation was deemed as not sufficient enough to use monitored natural attenuation as the sole remediation method at the site.

***Keywords**: Compound-specific isotope analysis, groundwater contamination, chlorinated solvents, PCE, TCE, cDCE, VC, biodegradation, reductive dechlorination*

Table of contents

1 Introduction

1.1 Aim of study

The aim of the study is to analyse groundwater samples, using compound-specific isotope analysis (CSIA), from a site contaminated with chlorinated solvents, specifically tetrachloroethylene (PCE) to answer the following questions: What are the spatial concentrations of PCE and its degradation products trichloroethylene (TCE), cis-1,2-dichloroethylene (cDCE) and vinyl chloride (VC)? Is degradation of contaminant compounds occurring and if so, is there any spatial variation? What factors are affecting the occurrence and the extent of degradation? Lastly, is the degradation extensive enough that monitored natural attenuation can be a remediation alternative?

1.2 Chlorinated solvents

Chlorinated solvents, also known as chlorinated aliphatic hydrocarbons, have been used as solvents and extractants in the electronic- and chemical industry as well as in dry cleaners. Tetrachloroethylene (PCE) and trichloroethylene (TCE) include two of the most used chlorinated solvents (Pankow & Cherry, 1996). Their usage peaked in the 1970s, where TCE accounted for half of all usage in Sweden (Naturvårdsverket, 2007).

Chlorinated solvents occur as dense non-aqueous phase liquids (DNAPLs), due to their higher density and viscosity lower than that of water. Their low viscosity combined with their high density increases their mobility, both in soil layers and in groundwater (Naturvårdsverket, 2007; Pankow & Cherry, 1996). These characteristics in combination allow them to accumulate on top of less permeable material. The low interfacial tension between chlorinated solvents and water causes dissolved solvents to infiltrate pores and fractures more easily, leading to deeper penetration and accumulation in the subsurface. Their low partitioning to soil material implies that they only weakly bind to bedrock and soil (Pankow & Cherry, 1996). As groundwater passes through, the chlorinated solvents can then be re-released through diffusion and spread almost as quickly as the groundwater velocity. Therefore, areas contaminated with chlorinated solvents are complex due to the difficulties related to localising and defining the contamination spread (Naturvårdsverket, 2007; Pankow & Cherry, 1996).

1.2.1 Degradation of tetrachloroethylene (PCE)

Through anaerobic reductive dechlorination, also known as hydrogenolysis, biodegradation of PCE can produce TCE, cis-1,2-dichloroethylene (cDCE) and vinyl chloride (VC), in the respective order (Aelion et al., 2009). Reductive dechlorination takes place when there is a supply of electron donors while the chlorinated solvents act as electron acceptors (Wiedemeier et al., 1996). It is a stepwise process where a chlorine atom is replaced by a hydrogen atom as illustrated in Figure 1. Although TCE can produce

trans-1,2-dichloroethylene and 1,1-dichloroethylene as well, cDCE is the predominant product of TCE reduction (Aelion et al., 2009).

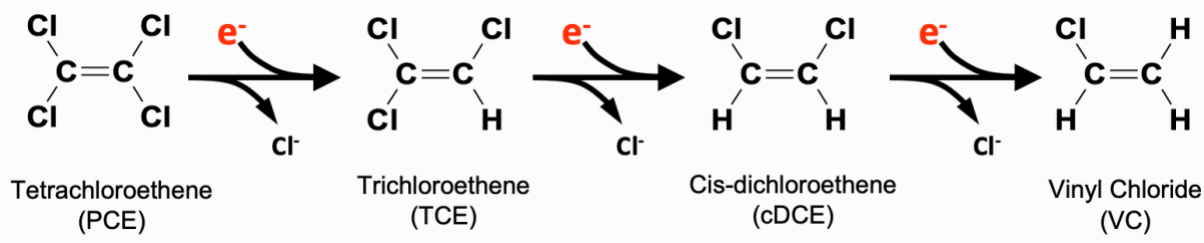

Figure 1. *Biodegradation of PCE to TCE, cDCE and VC through reductive dechlorination (Wanner, 2023).*

Biodegradation takes place under certain hydrochemical conditions and is a process that can transpire over a long period of time. Parameters that can be used as indications of favourable reducing conditions are the occurrence of methane and elevated concentrations of iron (Hunkeler et al., 2005). Other parameters that can be used include oxygen, nitrate and ammonia, sulphate, and sulphite as well as pH (Pankow & Cherry, 1996). Incomplete degradation can lead to accumulation of toxic degradation products such as VC. Due to these characteristics, chlorinated solvents are very persistent contaminants that can remain for hundreds of years and lead to extensive contamination plumes that are extremely difficult to clean up (Naturvårdsverket, 2007; Pankow & Cherry, 1996).

1.2.2 Health risks

Chlorinated solvents have negative effects on human health ranging from medium to very hazardous in severity depending on the type of chlorinated solvent. Additionally, there can be either long-term or short-term effects. There are several ways humans can be exposed to chlorinated solvents in groundwater, including direct contact, intake of contaminated water through drinking water or inhalation of fumes. Fumes can enter buildings by transport through the ground from a contamination plume (Naturvårdsverket, 2007).

The health effects of PCE include damage to the liver, kidneys, and the central nervous system. PCE is also suspected as a potential carcinogen (ECHA, 2022a; WHO, 2020). TCE and VC are both carcinogenic (ECHA, 2022b, 2023) while TCE also is a suspected mutagen (ECHA, 2022b; Naturvårdsverket, 2021). Due to these health risks, exposure to chlorinated solvents should be kept to a minimum. The guideline value for the sum of PCE and TCE in drinking water in Sweden is 10 µg/l (Naturvårdsverket, 2021). This value is based on the value by the European Chemicals Agency (ECHA) as part of the drinking water directive in the EU (ECHA, 2020).

1.3 Compound-specific isotope analysis (CSIA)

Analysing degradation by studying concentration changes between parent and daughter compounds alone can lead to inaccurate assumptions since many degradation products can be produced by various

parent compounds (Hunkeler et al., 2005). Analysing the compound-specific stable isotopes ratios (CSIA) offers a more extensive explanation for the biodegradation situation in contaminated groundwater (Aelion et al., 2009; Hunkeler et al., 2008). Stable isotopes are non-radioactive atoms with different numbers of neutrons, which differ in their masses (Aelion et al., 2009). During degradation, small variations in reaction rates between compounds with light and heavy isotopes lead to isotope fractionation where the degradation products are depleted in the heavy isotopes while the reactant, or parent compound, is increasingly enriched in the heavy isotopes (Hunkeler et al., 2005). In Figure 2 examples of TCE and cDCE with variations in isotopes are visualised. The combination of gas chromatography (GS), a combustion oven (C) and isotope ratio mass spectrometry (IRMS) enables analysis of isotope ratios for specific compounds (Aelion et al., 2009). Hence, CSIA can be used in combination with concentration analysis to obtain a more reliable result while also reducing the need for regular monitoring, which in turn can reduce the cost (Hunkeler et al., 2008).

Figure 2. *Conceptual model of chlorinated solvent consisting of heavy and light isotopes with the compounds cDCE, TCE and TCE from left to right (Wanner, 2023).*

1.3.1 CSIA of Carbon

The carbon isotopes ^{12}C (light isotope) and ^{13}C (heavy isotope) are stable and can be analysed from degradation of PCE where their proportions are measured for samples using mass spectrometry. Values of $\delta^{13}C$ in permill (‰), are calculated for each individual compound using the equation in Figure 3 (Aelion et al., 2009; Baskaran, 2012). A shift of the parent compound to higher (less negative) $\delta^{13}C$ values is an indication of degradation, whereas the resulting product will have lower (more negative) values. A method to estimate the original $\delta^{13}C$ value for PCE in a contaminated aquifer is to use the most negative $\delta^{13}C$ value detected (Hunkeler et al., 2008).

$$\delta^{13}\mathrm{C} = \left(\frac{\left(\frac{^{13}\mathrm{C}}{^{12}\mathrm{C}}\right)_{\mathrm{sample}} - \left(\frac{^{13}\mathrm{C}}{^{12}\mathrm{C}}\right)_{\mathrm{standard}}}{\left(\frac{^{13}\mathrm{C}}{^{12}\mathrm{C}}\right)_{\mathrm{standard}}} \right) \times 1,000‰$$

Figure 3. *Equation used to calculate the $\delta^{13}C$ value using the carbon isotope ratio value (R) of the sample and of the standard (Baskaran, 2012).*

1.3.2 Defining the degradation

Isotope data can be evaluated with the Rayleigh equation in Figure 4 to estimate the extent of degradation. This can be used to determine if the nature of the degradation is extensive enough to implement monitored natural attenuation as the remediation method (Aelion et al., 2009).

$$\delta^{13}C = \delta^{13}C_0 + \varepsilon_{bulk}(‰) \times \ln f_{DEG}$$

***Figure 4**. Simplified Rayleigh equation. f_{deg} = fraction of compound not yet degraded, C/C_0, where C is the instantaneous concentration and C_0 is the initial concentration of the chlorinated solvent. ε_{bulk} is the isotope enrichment factor, a form of quantification of the isotope fractionation (Aelion et al., 2009).*

Furthermore, the equation can be used to construct a Rayleigh correlation, called a Rayleigh plot. The Rayleigh plot predicts that the function of $\delta^{13}C$ (y-axis) should be a straight line on the natural logarithm of the remaining concentration (x-axis) if the isotope fractionation is due to degradation. The slope of the degradation line is given by the isotope enrichment factor (ε_{bulk}). If it does not follow a straight line, dilution, dispersion, volatilisation, or sorption may instead be the reason for the varying isotope values. Additionally, the Rayleigh equation cannot be applied to intermediate degradation products, for example TCE, since they are being produced and degraded simultaneously (Hunkeler et al., 2008).

1.4 Site description

Blekingegatan is a former dry-cleaning site, contaminated with chlorinated solvents. Continuous investigations have been conducted to monitor concentration levels of PCE and degradation products in groundwater collected from installed multi-level system wells (Sweco, 2023). This project is in collaboration with SWECO and the Morwick G360 Groundwater Research Institute from Guelph, Canada and was assigned by Sweden's Geological Survey (Sveriges Geologiska Undersökning) (SGU, 2020).

1.4.1 Historical background

The site is located at Blekingegatan 19, Helsingborg, in a residential area with current property designation "Räven 57 and Räven 58" (Figure 5). Between 1929 to 1970 the dry cleaner "Otto Borg Kemiska" was active at the site, and in 1933 a closed facility for washing with PCE was installed. "Rektorns kemiska tvätt- & presstjänst" took over the business in 1970 to permanently close in 1979. The washing machines are believed to have been situated in the eastern part of the western building, but the type of washing liquid used remains unknown. In 1979 the building was removed, and residential houses were built on the old property (Sweco, 2011; WSP, 2015).

***Figure 5**. Orthophoto from 1960 of Blekingegatan, provided by ©Lantmäteriet and modified in QGIS.*

1.4.2 Hydrogeological conditions

The bedrock below the site is part of the "höganäsformation", consisting of alternating layers of fine-grained sandstone, mudstone, heterolith and coal. The upper bedrock consists of sandstone that has a varying thickness of 5 to 15 metres. The first upper 6.2 metres of the sandstone is severely weathered and fractured (Sivhed, 2020). In the lower part of the sandstone, layers of medium to coarse sand have been encountered. A heterolith underlies the sandstone, often characterised by a clay filled upper layer and sand deeper down. Additionally, only some of the fractures in the ground are assumed to originate from before drilling was conducted at the site (Sivhed, 2021). The investigated site is situated at a height, around 37-43 metres above sea level, sloping towards the southwest (WSP, 2015). The depth to the water table at the source zone is approximately 8-9 metres while it is 4-5 metres 80-100 metres downstream from the source (Sivhed, 2020; WSP, 2015).

Due to the geological and hydrogeological conditions the water carrying capacity of the bedrock has been divided into 3 water conducting units: aquifer 1, 2 and 3 (Figure 6). Aquifer 1 is an unconfined aquifer in the sandstone 10-18 metres below the surface. It is characterised by high porosity and high hydraulic conductivity. Aquifer 2 is confined in the heterolith down to 35-45 metres below the surface with porosity mainly due to fractures. The permeability can be high in brittle areas. Aquifer 3 is confined in solid fractured sandstone with porosity due to fractures and with high permeability. Additionally, the average hydraulic conductivity of the aquifers is estimated to approximately $3 \cdot 10^{-5}$ m/s with groundwater flowing primarily in the southwest direction. The horizontal permeability is generally higher than the vertical permeability. This applies both to the upper and lower parts of the reservoir (WSP, 2015).

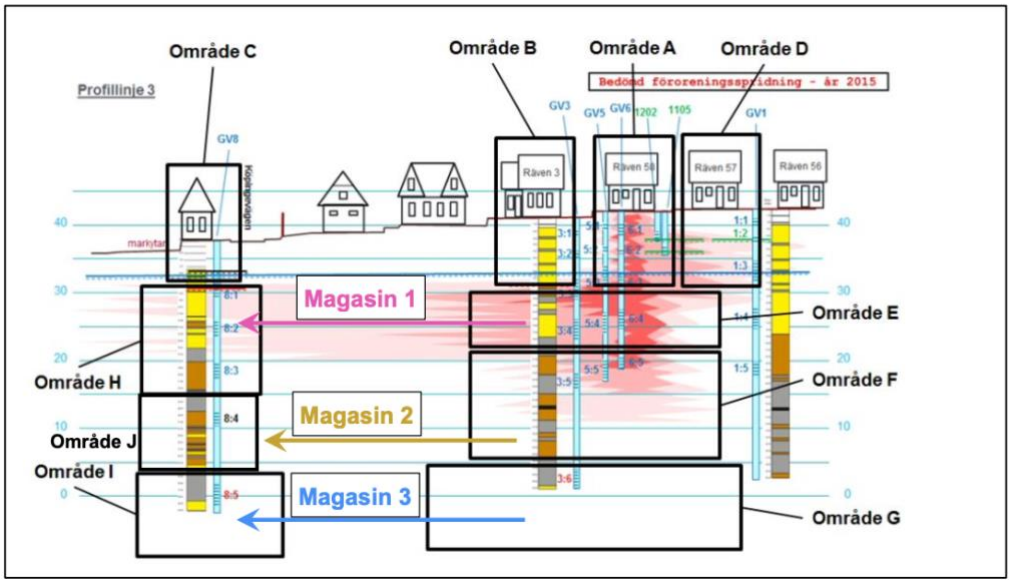

Figure 6. *Conceptual model of site subsurface profile with aquifer 1, 2 and 3 (indicated as Magasin 1, 2 and 3, respectively). The profile has been further divided into separate control areas (områden) from A to J to distinguish downstream from source and as well as at different depths (WSP, 2015).*

The closest water recipient is the marine harbour 1400 metres away from Blekingegatan (Sweco, 2011). In the Helsingborg area the sedimentary bedrock offers a good water supply and a few of these are being utilised some distance away from the site. One of the communal old deep bedrock wells, located 700-800 metres west of the site, is still used by the hospital. The well is acting as a water resource reserve and is utilised for technical purposes. Moreover, 3 kilometres southwest of the site the water protection area of Ramlösa is situated, 4.5 kilometres southeast of the site is the water protection area of Örbyfältet and 7 kilometres northeast of the site, the water reservoir of Holks is located (SGU, 2019; Sweco, 2011).

1.4.3 Previous investigations

Blekingegatan was classified as a risk class 1 contaminated site due to the long period of emissions, the high hazard of PCE and the high sensitivity of the site as it is currently a residential area. The classification was given by the County Board of Skåne during a MIFO phase 1 inventory, a standardised method for inventing contaminated areas (Sweco, 2011). The site has been continuously investigated since 2011, confirming the contamination of both the saturated and the unsaturated zone. Contaminants that have penetrated the saturated zone are estimated to have led to further contamination downstream in the direction of the groundwater flow, creating a contamination plume, illustrated in the conceptual model in Figure 7 (SGU, 2020; WSP, 2015).

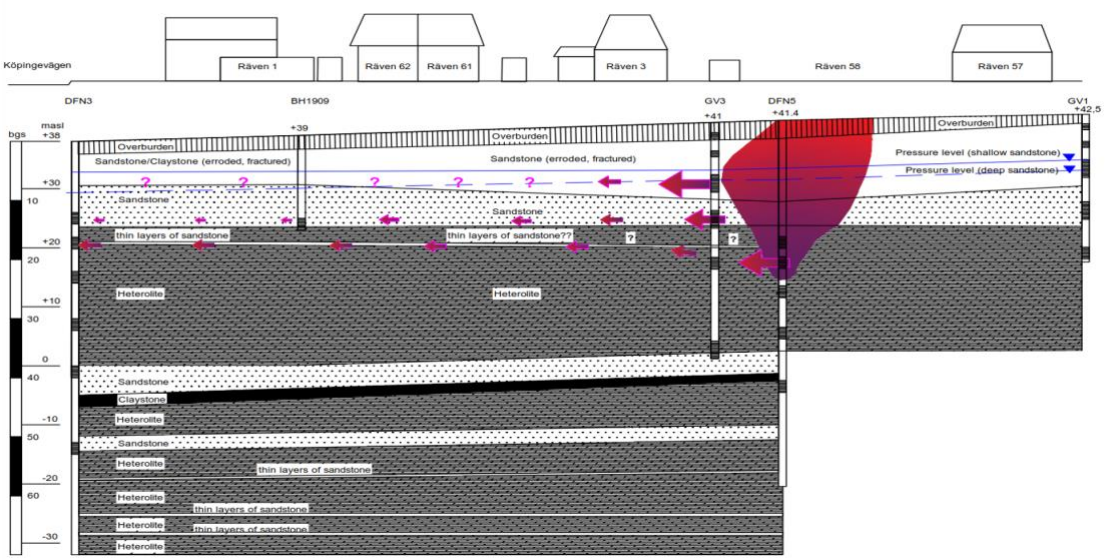

Figure 7. *Conceptual model of profile longsect with contamination source, contamination plume and groundwater flow moving downstream (towards the left-hand side) from the source zone (right hand side). Model provided by SWECO®.*

Figure 8 displays the 16 installed multi-level system (MLS) wells that make it possible to sample pore gas and groundwater on different ground levels. DFN1-5 were installed in 2019 and DFN6-16 were installed in 2021 (Sweco, 2021). The installation was conducted with the aim of using the discrete fracture network (DFN) approach; a method specifically developed for investigations of contaminants in sedimentary bedrock which includes investigations of the bore hole, the rock core, the groundwater, the hydrogeological properties, and the contaminant situation (Parker et al., 2012; Sweco, 2021). There is, however, evidence that concentrations in the deeper well filters decrease with time, raising the question of whether the spread of contaminants has occurred as a result of drilling and installing the MLS wells (Sweco, 2022c).

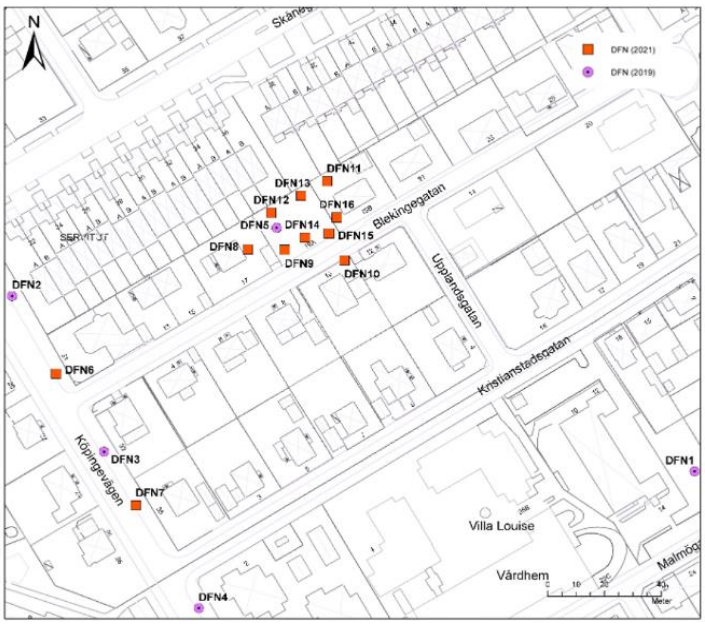

Figure 8. *Map of Helsingborgsgatan with the 16 MLS wells, DFN1 to DFN16. The pink circles represent the wells installed in 2019 and the orange squares represent the wells installed in 2021. Map provided by Sweco®.*

The criteria for drinking water have been followed as a guideline in the investigations, where the total concentration of PCE and TCE should not exceed 10 µg/l 50 metres downstream from the source and down to reservoir 3, 35-40 metres below the surface. From this criteria, site-specific guideline values have been calculated for the different control areas (Figure 6), which are 2000 µg/l in E, 500 µg/l in H, 20 µg/l in G and 10 µg/l in I. The guideline values are presented in Table 1 together with the highest measured total values of PCE and TCE (Sweco, 2022a).

Table 1. *Highest values (Högsta uppmätta halt) of total PCE and TCE measured in the control areas (Kontrollområde), compared to the site-specific guideline values (Riktvärde GV) in µg/l. The values in the table are the result from the latest sampling occasion on the condition that several samples have been collected at the same depth at the same time. The second column indicate the number of samples gathered (Antal prov) (Sweco, 2022a).*

Kontroll-område	Antal prov	Högsta uppmätta halt av summa PCE och TCE	Riktvärde GV summa PCE och TCE
E	47	76 000	2 000
H	23	4 800	500
G	3	120	20
I	6	14	10

Overall, the contamination in the ground has been estimated to reach a depth of 40 metres. Concentrations of up to 10-50 mg/l of PCE and 1-10 mg/l of TCE have been recorded between a depth of 9-20 metres. In the unsaturated zone, 50-1000 mg/l and 10-500 mg/l of PCE and TCE, respectively, have been measured (SGU, 2019, 2020). Also, investigations of indoor air in buildings on the old property were conducted from 2012 to 2014. The results showed elevated concentration of primarily PCE but also TCE, reaching concentrations of 379-620 µg/m^3 for PCE and 10-32 µg/m^3 for TCE. These are values that surpassed the target value of 10 µg/m^3 during measurements (Mattisson et al., 2012; WSP, 2015).

1.4.4 Risks and measures

A risk evaluation of the site was conducted in the main study by WSP (2015) from which the following could be concluded:

- Elevated concentrations of chlorinated solvents indoors pose a risk to human health.
- Low, yet possible, risk of direct contact with contaminants at surface.
- The long-term effects of the contamination can be estimated as being low to medium, both to humans and to the environment.
- The levels exceed the guideline values for drinking water and thus, the potential long term negative effects on the groundwater as a natural resource cannot be ignored.

Hence, it was assessed that the contaminated site requires risk reduction to ensure safe concentration levels in the area; ideally, a 90-99% reduction in the source zone would suffice (WSP, 2015).

1.5 Monitored natural attenuation

Monitored natural attenuation (MNA) is a remediation method that uses natural attenuation processes, for example biodegradation, to reduce the risk level of contaminated sites. This method can be effective when natural processes result in sufficient contamination decreases within an acceptable time period compared to other remediation alternatives. MNA can sometimes be combined with other remediation methods to further increase the efficiency of the remediation (Wiedemeier et al., 1996). Moreover, it is common that different remediation methods are used for the plume and for the source zone. However, measures of remediation to reach initial concentration levels previous to the contamination is rarely possible (Naturvårdsverket, 2007).

2 Method

2.1 Sampling preparations

In preparation of the sampling campaign for this study, equipment was assembled, including 120 glass vials of 40 ml with lids, gloves, protective glasses, coolers, and iron test strips for Fe^{2+} field measurements. Prior to sampling, the vials were placed in an oven at 80°C for 24 hours to remove any potential occurrence of volatiles whereafter they were labelled.

2.2 Groundwater sampling

Groundwater sampling took place at Helsingborgsgatan site from 20th to 23rd of March 2023. The investigation was in parts conducted in accordance with the field manual from SGF (2013). Samples were collected from 9 multi-level system wells and included a total of 34 sampling levels. Figure 9 displays the MLS wells included in the sampling which were DFN3, 5, 6, 8, 9, 11, 12, 13, and 15.

Figure 9. *Map of Helsingborgsgatan, the contaminated area, with the sampled wells, the profile longsect and transects. The map was constructed in QGIS with ©Google Satellite as the base map.*

Prior to collecting the samples, groundwater levels were measured with a water level metre and three times the well volume was purged to avoid sampling stored well water. Field parameters were measured

and documented using a multi-parameter probe wired to a flow cell (YSI ProDSS) after the values had stabilised. The measured field parameters included temperature, pH, specific conductivity, oxidation-reduction potential and dissolved oxygen.

The groundwater sampling of each well was conducted from least to most contaminated port to minimise the risk of cross contamination. The sampling order was based on concentration data gathered from previous years by Sweco (Sweco, 2022b). In addition, equipment was cleaned with distilled water in between each sampling occasion. Groundwater was pumped from the wells using one of the following pumps: peristaltic pump, double valved pump, bladder pump or waterra pump (Figure 10). The pump was connected to polyethylene tubing.

Figure 10. Set-up of waterra pump during purging of groundwater in DFN9.

At each sampling point the Fe^{2+} concentration was measured with a test iron strip before 3 glass vials of 40 ml were collected for CSIA. The vials were top filled to avoid air bubbles and labelled with a specific number, the date, and the sampling point. Sweco was responsible for conducting the sampling of groundwater for concentration analysis. Samples for chlorinated solvent concentration analysis were collected in dark 40 ml glass vials with a preservative, samples for iron and manganese analysis in 250 ml bottles and samples for cations and anions in 60 ml bottles. A more detailed description can be found in the report by Sweco (2023). All samples were stored in coolers directly after sampling and during transport. The concentration samples were sent for analysis to the accredited lab ALS Scandinavia and more information about their procedures can be found on their web page (ALS, n.d).

Some irregularities occurred during sampling. In DFN13.6 the tubing was dropped down the pipe and no samples could be retrieved. In ports DFN13.3, DFN13.4, DFN15.3 and DFN15.4 no samples could be gathered due to the groundwater volume being too low. As a result, samples were gathered from DFN12.4 and DFN12.6 instead. Furthermore, in DFN9.5 less than three well volumes were purged before sampling due to low groundwater volumes, and in DFN11.2 air bubbles emerged in the tubing during sampling. During transport to the laboratory 4 samples for iron and manganese concentrations were destroyed. These included DFN3.1, DFN3.2, DFN5.2 and DFN5.5.

2.3 Conducting CSIA

The compound-specific isotope analysis was conducted at the department for Earth Science at Gothenburg University in Gothenburg. The analysis was conducted for PCE, TCE, and cDCE after results of the investigated concentrations had arrived from ALS. During this time the samples had been stored in a cooler in the department. CSIA was not conducted for VC due to the low concentrations detected.

The samples were diluted to identical concentrations of 300 µg/l to increase the precision of the analysis. Samples with concentrations already lower than this were measured undiluted. The samples were then injected with a CombiPal Autosampler (CTC Analytica, Zwingen, Switzerland) into the GC (Agilent 7890A) from the headspace of 20 ml vials. The vials were filled with 15 ml of the sample solution. After injection, the compounds were separated in the GC by maintaining the temperature at 50°C for 2 minutes before increasing it with 5°C per minute until a temperature of 150°C was reached. A DB-VRX column (60 m, 0.25 mm, 1.40 µm, Agilent) was used for the separation with a helium flow rate of 1.2 ml per minute. After separation, the compounds passed through the combustion reactor (GC5, Elementar Isoprime) where they were converted into CO_2. Figure 11 displays the set-up of the equipment devices. Afterwards the ratio of $^{13}CO_2$ and $^{12}CO_2$ could be determined in the IRMS (Elementar Isoprime). This was done in relation to a reference CO_2 being used as standard, the standard being the international Vienna Pee Dee Belemnite standard with the value 0.0112372 (Aelion et al., 2009; Hunkeler et al., 2008). The $\delta^{13}C$ values could then be calculated according to the equation in Figure 3 for each analysed compound. The measurements for each sample point were replicated 3 times and a mean value was calculated as the final $\delta^{13}C$ value. Lastly, an uncertainty evaluation was included for the values in the form of the standard deviation of the mean. Due to the detection limit being approximately 60 µg/l, CSIA could not be conducted for some of the samples with concentrations lower than this.

Figure 11. *Set-up during CSIA with, a) combustion reactor to the left, gas chromatograph to the right and autosampler on top, b) the isotope ratio mass spectrometer.*

2.4 Data analysis

The data analysis consisted of two main parts, 1) visualising the concentration and isotope data by constructing profiles of the longsect and transect of the site with value indications, 2) constructing a Rayleigh correlation in the form of a plot displaying the nature of the changes in the isotope data. In addition to this, field parameters and parameters affecting reducing conditions were compared between the source zone and the downstream area briefly.

2.4.1 Profile diagrams of the subsurface

Microsoft Excel and PowerPoint were used to construct 2-dimensional profile diagrams for concentrations of PCE, TCE, cDCE and VC as well as for isotope $\delta^{13}C$ values for PCE, TCE and cDCE. Figure 9 shows the three profiles displayed in the diagrams; a longsect of the contamination plume including the MLS wells DFN6, 8, 9, 5, 12, 13, 15 and 11 in the respective order, a transect of the source zone including DFN12, 5, 8 and 9 in the respective order, and a transect 80 metres downstream from the source including DFN6 and DFN3. This resulted in a total of 21 separate ground profile diagrams. Local topography and differences due to the wells not being completely linear to the longsect and transects were not adjusted for in the diagrams.

2.4.2 Rayleigh plot

The Rayleigh equation (Figure 4) was used to construct a Rayleigh plot in Microsoft Excel. The value used for the initial concentration, C_0, was 200 000 µg/l. This value approximately corresponds to the PCE solubility limit (WHO, 2020). Furthermore, the highest detected concentration at the site was 178 000 µg/l in 2019, a value close to the solubility limit justifying the usage of 200 000 µg/l for C_0. For the isotope enrichment factor (ε_{bulk}) the value -10.8‰ was used as it is the average ε_{bulk} value for PCE (Wanner et al., 2016). Thus, -10.8 corresponds to the slope of the degradation while the value 0 corresponds to the slope of dilution. The value used for $\delta^{13}C_0$ was -25.73‰ as an approximation for the isotopic signature of the source as it was the most negative value detected for PCE.

3 Results

3.1 Field and redox affecting parameters

No major differences were detected between the source zone and the downstream area for most of the field parameters and parameters affecting reducing conditions. These included temperature, specific conductivity, pH, dissolved oxygen, iron concentrations, nitrate, and sulphate. What did stand out was the redox potential. Much lower values were detected downstream compared to the source zone. The average values of DFN3 and DFN6 were -124.4 mV and -87.9 mV, respectively. In the source zone the overall average of the redox potential was -30.2 mV, however, DFN5 was the exception with an average of -87.8 mV. The methane concentrations differed between the source zone and the downstream area as well. The average methane concentration was 1310.9 µg/l and 967.9 µg/l for DFN3 and DFN6, respectively. The wells in the source zone had average methane concentrations of up to 4.5 µg/l, except for DFN5 with an average concentration of 650.3 µg/l.

3.2 Concentration data of chlorinated solvents

Figures 12 to 17 illustrate the chlorinated solvent concentration maps along a cross and long section at the site. It is important to note that the concentration maps are interpretations and not perfect presentations of reality. The wells are not exactly linear and measurements between the wells are approximations, furthermore the topography and the inclination towards the downstream area were not adjusted for in these diagrams.

Concentrations of up to 35500 µg/l of PCE were measured with the highest concentrations detected in the source zone, specifically in DFN9 and DFN8 (Figure 12). Note that concentrations in the source zone were up to 50 times, or more, higher than that of the concentrations in DFN6 downstream. The highest concentrations in the longsect were detected at a depth of 10 to 20 metres below the ground surface.

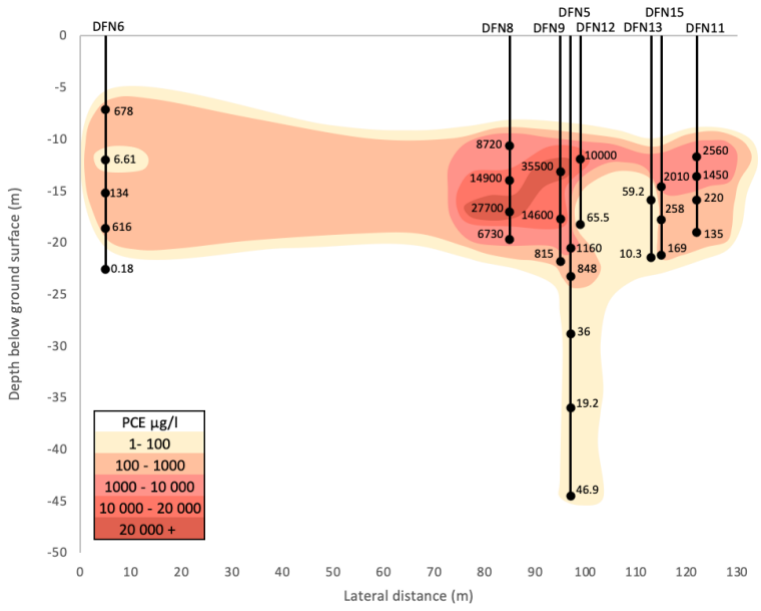

Figure 12. *Longsect concentration map of contamination plume with concentration data of PCE in µg/L.*

Figure 13a displays the higher concentrations that were detected towards the right-hand side of the source transect, at the southern or front part of Räven 58 property. Downstream, DFN6 had higher concentrations than DFN3 with the highest concentration being 678 µg/l (Figure 13b).

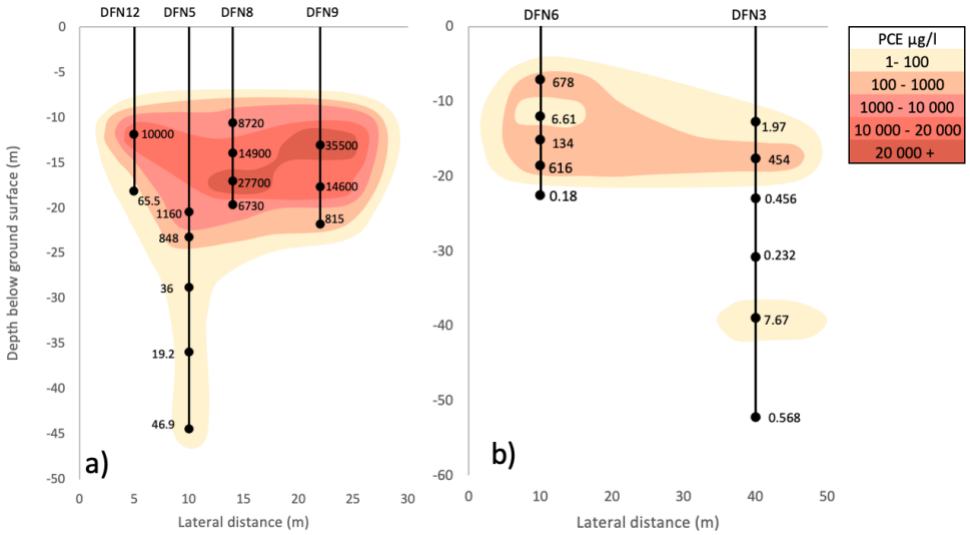

Figure 13. *Transect concentration map, of a) source zone and b) downstream 80 metres from the source, of contamination plume with concentration data of PCE in µg/l.*

The highest detected concentration of TCE was 13500 µg/l in DFN9 (Figure 14). Similarly, for TCE the highest concentrations were found in the source zone in DFN9 and DFN8 at a depth of 10 to 20 metres in the longsect.

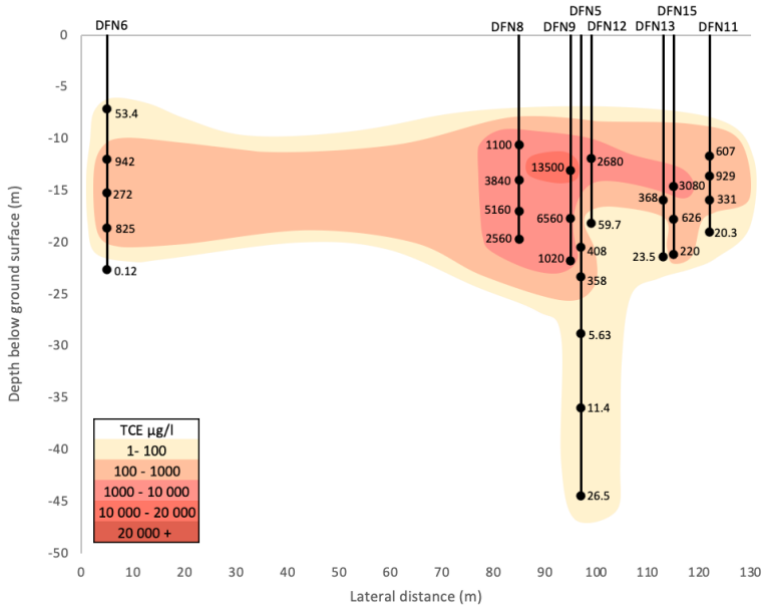

Figure 14. *Longsect concentration map of contamination plume with concentration data of TCE in µg/l.*

Figure 15a shows that the higher concentrations of TCE were detected towards the right-hand side of the source transect as well. Downstream, the highest measured TCE concentration was 942 µg/l,

measured in DFN6 (Figure 15b). Note that the concentrations downstream in DFN3 and DFN6 were generally higher for TCE than for PCE.

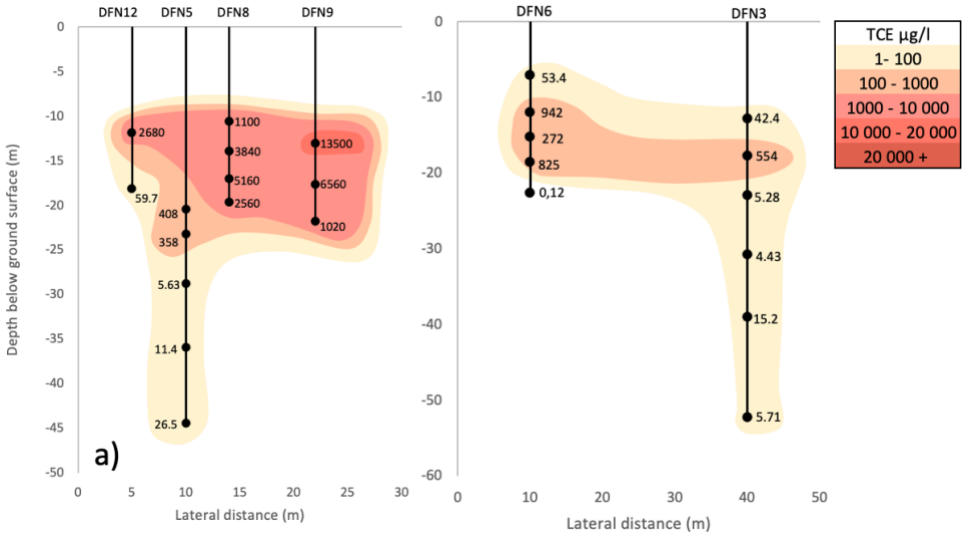

Figure 15. *Transect concentration map, of a) source zone and b) downstream 80 metres from the source, of contamination plume with concentration data of TCE in µg/l.*

Concentrations of cDCE were measured with the highest concentrations again detected in the source zone in DFN8 and DFN9, reaching a concentration of 1740 µg/l (Figure 16a). Figure 16b displays DFN3 with the highest measured concentration downstream of 152 µg/l. Similarly, the higher concentrations mainly occurred between 10 to 20 metres below ground surface. Note that the cDCE concentrations generally were observed to be lower than the TCE concentrations.

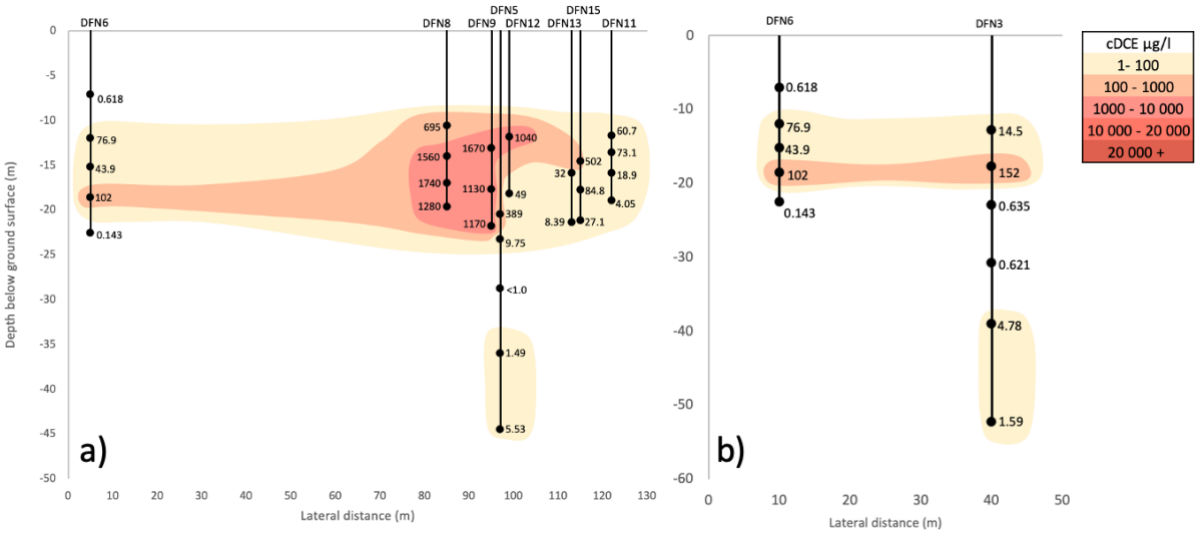

Figure 16. *Concentration map of, a) longsect of plume and b) transect 80 metres downstream from source, with concentration data of cDCE in µg/l.*

In contrast to PCE, TCE and cDCE, considerably lower concentrations of VC were detected. Figure 17 illustrates that higher concentrations were measured downstream rather than in the source zone. DFN6 had the highest concentration, 6.64 µg/l, downstream (Figure 17b). Again, at a depth of 10 to 20 metres.

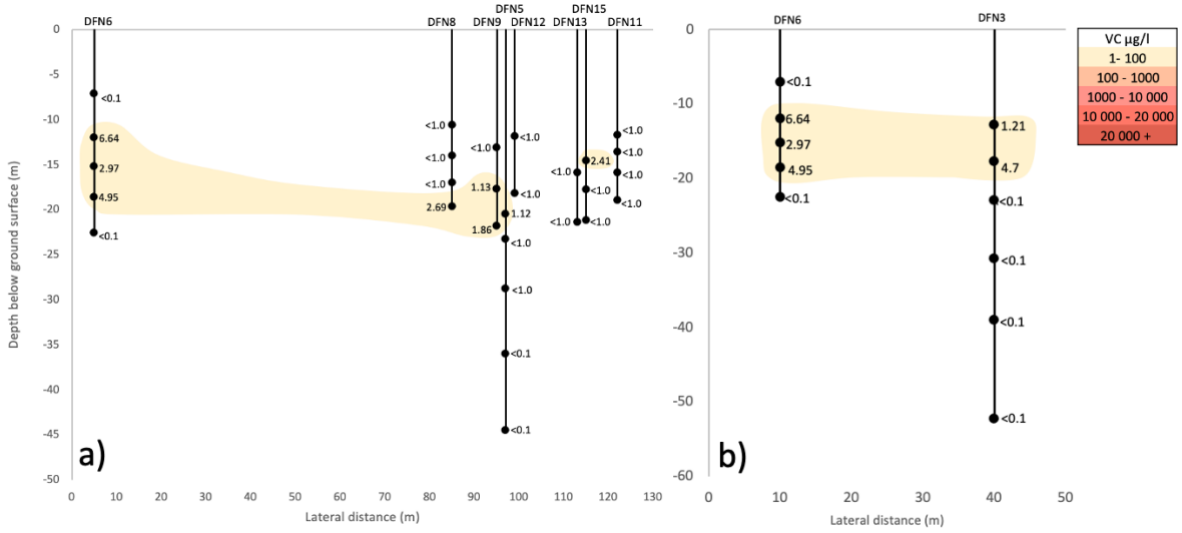

Figure 17. *Concentration map of, a) longsect of plume and b) transect 80 metres downstream from source, with concentration data of VC in µg/l.*

3.3 Isotope data

The $\delta^{13}C$ values for PCE ranged from -25.73‰ to -19.94‰ with an average standard deviation of 0.12‰. Figure 18 shows the longsect of the plume with the highest (least negative) values, of up to -20.37‰, measured in DFN6 and DNF15. DFN8 had the lowest values in contrast to the other wells. Like the concentration data, the highest detected $\delta^{13}C$ values were at a depth of 10 to 20 metres.

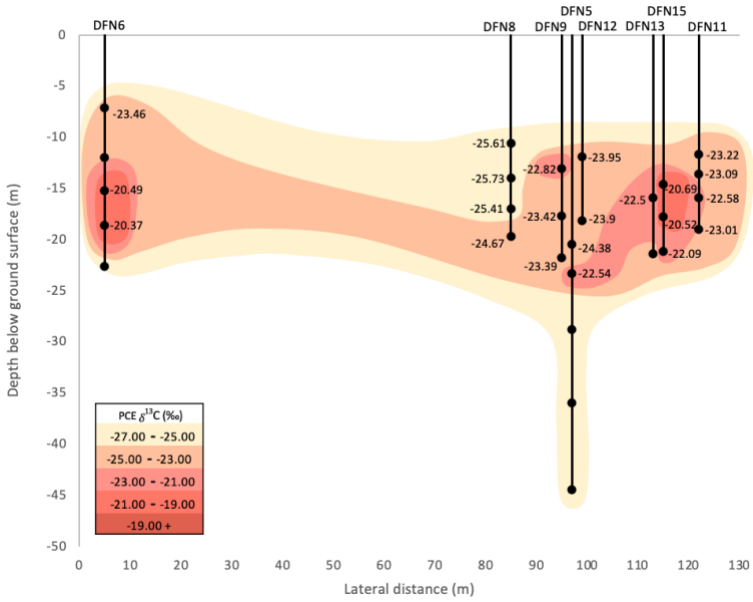

Figure 18. *Longsect-map of contamination plume with isotope data ($\delta^{13}C$) of PCE in ‰.*

Figure 19 displays a) the source transect and b) the downstream transect where the highest $\delta^{13}C$ value, -19.94‰, was detected in DFN3. Note that the downstream wells had higher (less negative) values than those in the source zone.

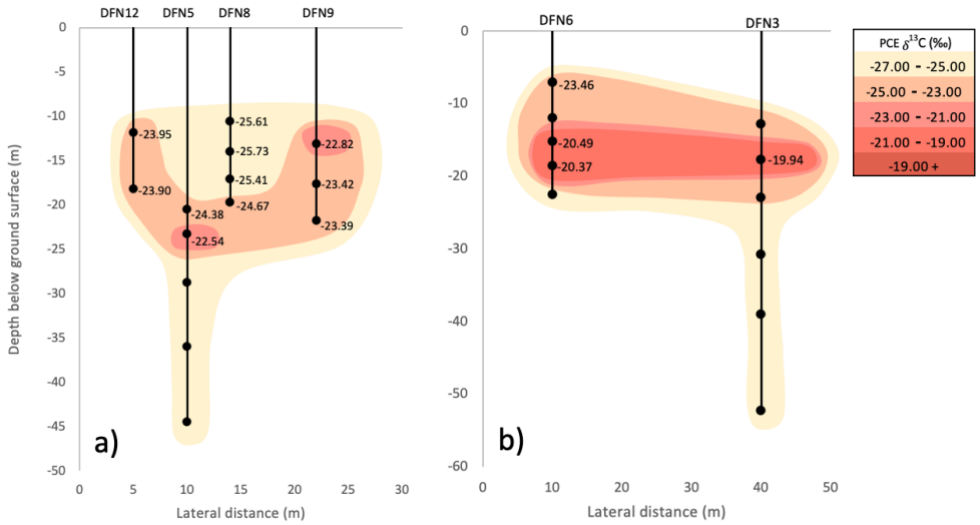

Figure 19. *Transect ground profile, of a) source zone and b) downstream 80 metres from the source, of contamination plume with isotope data ($\delta^{13}C$) of PCE in ‰.*

The $\delta^{13}C$ values of TCE ranged from -27.09‰ to -19.55‰ with an average standard deviation of 0.14‰. The highest values were detected in the source zone in DFN15, visible in the longsect (Figure 20). The $\delta^{13}C$ values of TCE were observed to be generally higher (less negative) than the $\delta^{13}C$ values of PCE.

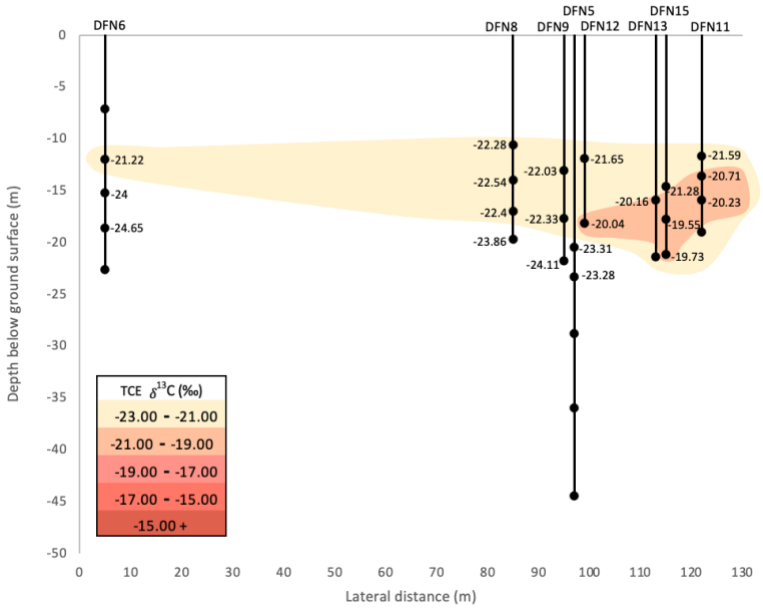

Figure 20*. Longsect map of contamination plume with isotope data ($\delta^{13}C$) of TCE in ‰.*

Figure 21 displays the exception to this where in a) the source zone, low values such as -23.28‰ and -24.11‰ were detected in DFN5 and DFN9, respectively, below a depth of 20 metres. In b) the downstream area, values as low as -24.00‰ and -24.65‰ were measured in DFN6 and -27.09‰ in DFN3 at a depth below 15 metres.

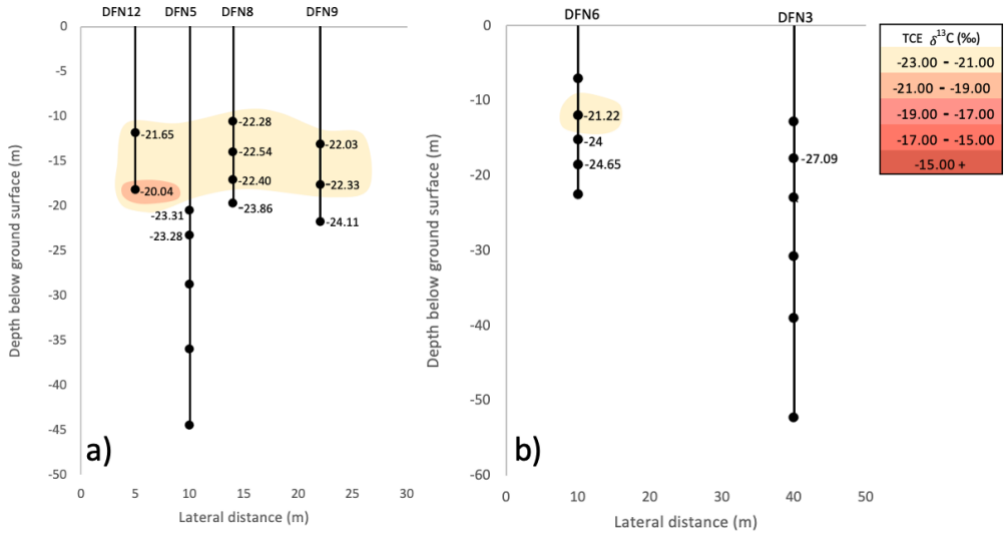

Figure 21. *Transect map, of a) source zone and b) downstream 80 metres from the source, of contamination plume with isotope data ($\delta^{13}C$) of TCE in ‰.*

The measured $\delta^{13}C$ values of cDCE had a range from -25.72‰ to -22.43‰, with the lowest value, -25.72‰, detected in DFN15 (Figure 22a). Note that all $\delta^{13}C$ values of cDCE in the source zone were lower (more negative) than the corresponding values of TCE in the source zone. Additionally, the cDCE values downstream (Figure 22b) were instead higher (less negative) than the corresponding values downstream of TCE. The average standard deviation was 0.14‰ for cDCE.

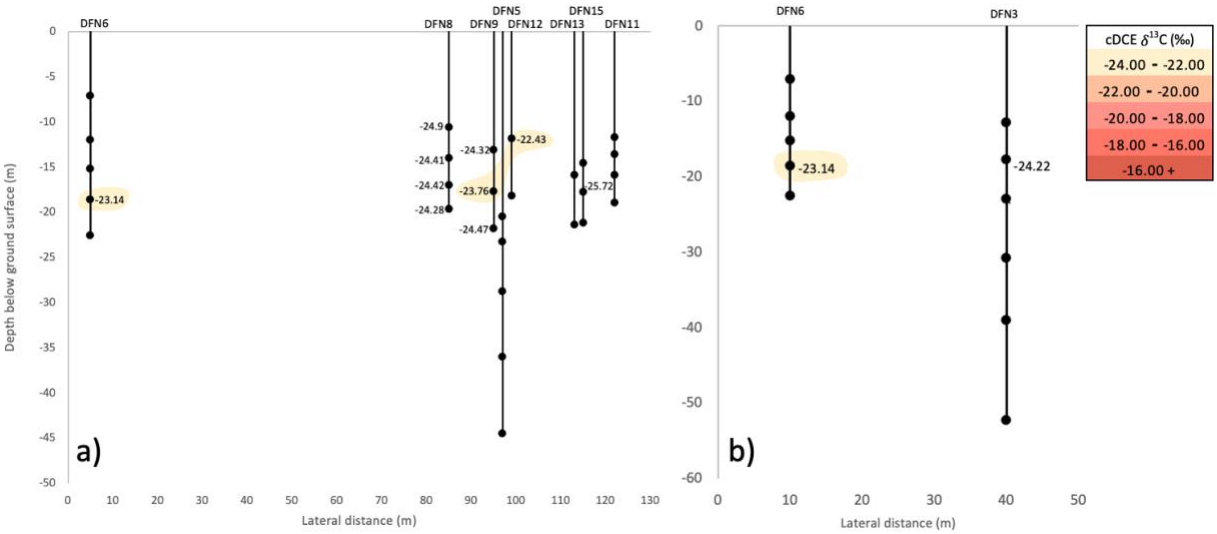

Figure 22. *Ground profile of, a) longsect of plume and b) transect 80 metres downstream from source, with isotope data ($\delta^{13}C$) of cDCE in ‰.*

3.4 Rayleigh plot

Figure 23 displays the potential development of isotope fractionation during either complete degradation (red line) or during complete dilution (black dotted line). Note that the plotted $\delta^{13}C$ values of PCE for both the source zone and the plume (downstream) displays an inclination towards the dilution line.

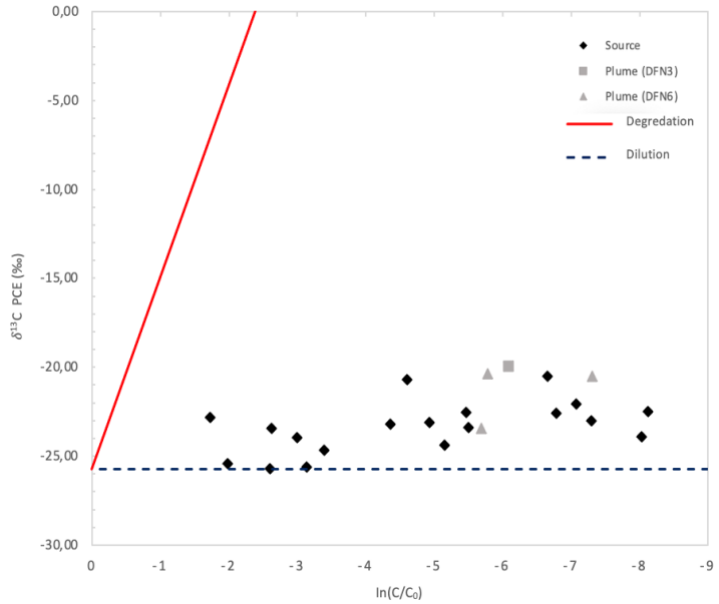

Figure 23. *Rayleigh plot with isotope data ($\delta^{13}C$) of PCE. The red line is an indication of the change in $\delta^{13}C$ that would occur if only degradation was taking place. The black dotted line indicates the change during dilution only.*

4 Discussion

4.1 Variations in redox potential and methane concentrations

The lower (more negative) redox potential measured downstream compared to in the source zone indicates more reducing conditions in the downstream area. This is reinforced by the elevated methane concentrations measured downstream as well. DFN5 is the exception in the source zone with low redox potential and elevated methane concentrations similarly to in the downstream area. DFN3 and DFN6 downstream as well as DFN5 in the source zone thus indicate favourable conditions for degradation for chlorinated solvents acting as electron acceptors.

4.2 Analysis of chlorinated solvent concentrations

There are indications of degradation taking place due to the presence of PCE and the degradation products TCE, cDCE as well as VC with PCE having the highest overall concentration whereby TCE had the second highest, cDCE the third highest and VC the lowest. The exception to this were the TCE concentrations of up to 942 µg/l in the downstream area (Figure 15) which were higher than the PCE concentrations of up to 678 µg/l (Figure 13). Something that could be a sign of more TCE being produced by PCE in the downstream area.

The highest concentrations of PCE, TCE and cDCE were all measured in the source zone while the concentrations downstream were lower, something that is in line with the nature of groundwater contamination plumes being more concentrated in the source zone. For VC, the downstream concentrations (Figure 17) were higher than in the source zone. This could be an indication that the degradation of cDCE is more extensive downstream, resulting in higher concentrations of produced

VC. However, the overall measured concentrations of VC were still very low compared to the other degradation products, suggesting that the degradation of cDCE to VC is limited.

Since assumptions of degradation cannot be made based solely on the measured concentration data (Hunkeler et al., 2005), it cannot be ruled out that these observed changes and patterns are a result of dilution. Furthermore, as brought forward in the report by Sweco (2022c), the higher concentrations of the chlorinated solvents may be due to mobilisation of the compounds during installation of the wells which over time decrease due to the flow of groundwater. Moreover, the report by Sivhed (2020) mentions that only some of the fractures in the bedrock are assumed to be from prior to the drilling. Thus, the installation of the wells may have resulted in more fractures in the bedrock and enabled mobilisation of the contaminants. When comparing the concentrations in DFN3, 5 and 6 that were installed in 2019 to the other DFN wells that were installed in 2021, it can be noted that the concentrations of the contaminants in DFN3, 5 and 6 are generally lower. Possibly a result of the concentrations having stabilised to a greater extent in the wells installed in 2019 than in the wells installed in 2021, which would be in accordance with the theory in the report by Sweco (2022c).

Other spatial variations of the contaminants include the higher concentrations detected toward the front of the property which approximately matches the placement of the old building in the orthophoto (Figure 5) with the suspected placement of the washing machines, and elevated concentrations (DFN8) directly downstream from the house. Additionally, the start of the higher concentrations at 10 metres down in the source zone coincide with the water table and continue down to a depth of 20 metres. This interval for the elevated concentrations is approximately the same as the interval for aquifer 1, which also is an aquifer with high porosity and high hydraulic conductivity. This could explain how the spread of elevated concentrations of the contaminants have been facilitated at this specific depth.

Furthermore, the measured concentrations of PCE and TCE from this sampling occasion exceed the site-specific guideline values for the different control areas E, H, G, and I, confirming that the contamination situation of the site still is severe and that measures are necessary to reduce the risk level of the site.

4.3 Analysis of isotope data and Rayleigh plot

When examining the $\delta^{13}C$ values of PCE and the accompanying degradation products one of the most pronounced deviations are the high (less negative) values of TCE. Since TCE is believed to be a degradation product of PCE, reductive dechlorination of PCE would be expected to result in lower (more negative) $\delta^{13}C$ values of TCE than that of the $\delta^{13}C$ values of PCE (Hunkeler et al., 2008). This is, however, not the case in the source zone, which suggests that TCE may instead be a primary contaminant, a parent compound, rather than a degradation product.

The lower $\delta^{13}C$ values, down to -27.09‰, of TCE downstream as well as furthest down in DFN5 and DFN9 (Figure 21) are signs that some TCE may be produced through degradation of PCE as well. This is reinforced by the high $\delta^{13}C$ values of up to -19.94‰ of PCE downstream (Figure 19), which suggests some form of degradation activity, and by the favourable reducing conditions in DFN3, 5 and 6 as indicated by the redox potential and methane concentrations. Moreover, this could explain the higher concentrations of TCE downstream (Figure 15) as perhaps originating from both the source zone and from reductive dechlorination of PCE. The lower $\delta^{13}C$ values of TCE observed at a depth of 20 metres and deeper in the source zone, specifically in DFN5 and 9, indicate that degradation is facilitated at depths greater than this. At this depth the bedrock type changes from sandstone into heterolith and mudstone, and a different aquifer, aquifer 2, is entered (Figure 6). With aquifer 2 being a closed system with high permeability mostly in the brittle areas, these changes in ground conditions may affect the potential for degradation. The lack of isotope data in the three lower ports of DFN5, however, limits our understanding of this to some extent.

When comparing the $\delta^{13}C$ values of cDCE (Figure 22) with the values of TCE (Figure 20) an assumption can be made that cDCE is produced mainly due to reductive dechlorination of primary TCE in the source zone. This would explain why the $\delta^{13}C$ values of cDCE in the source zone are lower than the values of TCE despite the values of TCE not being lower than the values of PCE. What is more is the low cDCE value at -25.72 ‰ in DFN15 compared to the high values of both PCE and TCE at -20.52‰ and -19.55‰, respectively, in DFN15, which strengthens this argument.

Downstream where the $\delta^{13}C$ values of cDCE are higher than for TCE it could be speculated that this is due to the magnitude of produced TCE from degradation of PCE being larger than the degradation of TCE to cDCE. Even though the isotope values of VC could not be investigated, again, the detected concentrations of VC indicate that some extent of degradation of cDCE to VC is going on, however, at a small scale. Ultimately, the average standard deviation values of PCE, TCE and cDCE were all within an acceptable range at 0.12‰, 0.14‰ and 0.14‰, respectively.

From the results of the Rayleigh plot (Figure 23) it can be concluded that a large part of observed concentration decrease is related to dilution rather than to degradation. Although some degradation is taking place, especially with the concentrations of cDCE and VC to support this, the degradation is not the main contributor to the change. Furthermore, from the measured results it would be difficult to quantify the exact rate of the degradation. With this increased knowledge of the contamination and the degradation at the site, it can be established that monitored natural attenuation would most likely not be a sufficient remediation method alone in the contaminated area.

4.4 Sources of error and limitations

During the sampling occasion different factors could have influenced the outcome of the result.
A primary factor being the lack of collected samples from some ports in several wells. This may have caused a gap in the concentration data and thus led to an incomplete representation of the concentration situation in the subsurface. Furthermore, although the equipment was cleaned, and tubing was changed in between every sampling occasion there is still a possibility that a small amount of water may have remained and led to cross contamination. The wells where air bubbles formed in the tubing and where not enough water was purged prior to sampling may have contributed to some unrepresentative concentration results as well. Additionally, although the samples were stored in coolers during transport and storage, it cannot be disregarded that the temperature may have fluctuated throughout. Any unforeseen factors affecting the samples during analysis at the accredited lab remain unknown.

Another challenge included interpreting the $\delta^{13}C$ values with several degradation products present and both PCE and TCE as potential parent compounds. According to Hunkeler et al. (2008), the presence of several parent compounds in groundwater can impede the detection of degradation pathways. Moreover, if continued emissions of contaminants with heavy isotopes occur in the source zone, this can lead to under detection of the actual magnitude of isotope fractionation caused by degradation (Hunkeler et al., 2008). There is a possibility that some of the degradation, especially of PCE, went unnoticed due to high concentrations of primary TCE altering the $\delta^{13}C$ values of TCE. Something that could have influenced the interpretations.

When it comes to the Rayleigh plot the most prominent uncertainty is the value used for the isotope enrichment factor (ε_{bulk}), which is an average for PCE and thus, the slope of the degradation line. In addition, Rayleigh plots were not produced with the $\delta^{13}C$ values of TCE, cDCE and VC due to them being intermediate degradation products. Therefore, it is of great importance to note that the created Rayleigh plot only displays the nature of the concentration change for the compound PCE.

The collective effect of the combined errors and limitations could have influenced the result in such a way where the precision of the defined contamination plume was affected. However, not to the extent where the results of the investigation should be disregarded or from which a different final conclusion could be defined. The most prominent outcome of a result without any limitations or errors would thus be a more detailed description of the concentration- and isotope data in the subsurface due to successful gathering of samples from all ports.

5 Conclusion

The measured $\delta^{13}C$ values from the conducted compound-specific isotope analysis indicate that degradation of PCE is taking place 80 metres downstream from the source in DFN3 and DFN6 as well as below a depth of 20 metres in the source zone in DFN5 and DFN9. However, the Rayleigh plot indicates that the observed concentration decrease is most likely due to dilution rather than to reductive dechlorination. The results of the compound-specific isotope analysis also suggest that some, although limited, degradation of TCE and cDCE is taking place, with a significant decline at cDCE, as indicated by the low concentrations detected of VC. Furthermore, there are indications that TCE, previously assumed to be a degradation product of PCE, may be part of the contamination source due to the detection of high $\delta^{13}C$ values of TCE with respect to the $\delta^{13}C$ values of PCE. From these results it can be concluded that sufficient degradation is not occurring in the overall contamination plume to rely solely on monitored natural attenuation as the remedial method. In order to reduce the risk level of the site, other measures would have to be considered which requires further investigation.

6 Acknowledgements

I would like to express my gratitude to Sveriges Geologiska Undersökning (SGU), especially Erik Bergstedt for assigning us this project and for their collaboration throughout this period. I would also like to thank Sweco Sverige AB and The Morwick 360 Groundwater Research Institute for their collaboration in this investigation and especially for their assistance at the time of sampling. Lastly, a special thanks to my supervisor Philipp Wanner who notified me of the project and who has assisted me through it.

7 Bibliography

Aelion, C. M., Höhener, P., Hunkeler, D., & Aravena, R. (2009). *Environmental isotopes in biodegradation and bioremediation* (1st ed.). CRC Press. https://doi.org/https://doi.org/10.1201/9781420012613

ALS. (n.d). *Om ALS Life Sciences - Sverige*. Retrieved 2023-08-21 from https://www.alsglobal.se/Om-ALS-life-sciences

Baskaran, M. (2012). *Handbook of environmental isotope geochemistry* (Vol. 1). Springer. https://doi.org/10.1007/978-3-642-10637-8

ECHA. (2020, December 23). *Quality Criteria for Drinking Water*. European Chemcials Agency. Retrieved 2023-07-25 from https://echa.europa.eu/sv/eu-drinking_water_recast-anx_i/-/legislationlist/details/EU-DRINKING_WATER_RECAST-ANX_I-100.298.317-VSK-G31WK9

ECHA. (2022a, December 16). *Substance Information. Tetrachloroethylene*. European Chemicals Agency. Retrieved 2023-07-25 from https://echa.europa.eu/sv/substance-information/-/substanceinfo/100.004.388

ECHA. (2022b, July 08). *Substance Information. Trichloroethylene*. European Chemicals Agency. Retrieved 2023-07-25 from https://echa.europa.eu/sv/substance-information/-/substanceinfo/100.001.062

ECHA. (2023, May 18). *Substance Information. Chloroethylene*. European Chemicals Agency. Retrieved 2023-07-25 from https://echa.europa.eu/sv/substance-information/-/substanceinfo/100.000.756

Hunkeler, D., Aravena, R., Berry-Spark, K., & Cox, E. (2005). Assessment of Degradation Pathways in an Aquifer with Mixed Chlorinated Hydrocarbon Contamination Using Stable Isotope Analysis. *Environmental Science & Technology*, *39*(16), 5975-5981. https://doi.org/10.1021/es048464a

Hunkeler, D., Meckenstock, R. U., Lollar, B. S., Schmidt, T. C., & Wilson, J. T. (2008). *A guide for assessing biodegradation and source identification of organic ground water contaminants using compound specific isotope analysis (CSIA) [electronic resource] / Daniel Hunkeler ... [et al.]*. Office of Research and Development, National Risk Management Research Laboratory, U.S. Environmental Protection Agency.

Mattisson, K., Tinnerberg, H., & Albin, M. (2012). *Miljömedicinsk bedömning angående inläckage av klorerade lösningsmedel från mark på tomt i Helsingborg, där det tidigare legat en kemtvätt.* (7). L. Skåne.

Naturvårdsverket. (2007). *Klorerade lösningsmedel - identifiering och val av efterbehandlingsmetod* (5663). Naturvårdsverket.

Naturvårdsverket. (2021). *Översyn av toxikologiska referensvärden för PCE och TCE*. Naturvårdsverket.

Pankow, J. F., & Cherry, J. A. (1996). *Dense Chlorinated Solvents and Other DNAPLs in Groundwater: History, Behavior, and Remediation*. Waterloo Press.

Parker, B., Cherry, J. A., & Chapman, S. (2012). Discrete fracture network approach for studying contamination in fractured rock. *AQUA mundi*, *3*, 101-116.

SGU. (2019). F.d. kemtvätt vid blekingegatan, Helsingborg. Information om pågående åtgärdsförberedelser, vid studiebesök av Nätverket Renare Mark Syn i oktober 2019. In: Sveriges Geologisk Undersökning.

SGU. (2020). *Före detta kemtvätt vid Blekingegatan, Helsingborg*. S. G. Undersökning.

Sivhed, U. (2020). *SWECO - Projekt blekingegatan, Helsingborg. Uppdatering av geologisk modell 2020-01-24*. N. G. AB.

Sivhed, U. (2021). *SWECO - Projekt Blekingegatan, Helsingborg. Borningarna DFN 6 - 16 Preliminär rapport*. N. G. AB.

Sweco. (2011). *Översiktlig miljöteknisk markundersökning (MIFO fas 2) vid f.d. kemtvätt på fastigheterna Räven 56-58, Helsingborgs kommun*. S. E. AB.

Sweco. (2021). *Blekingegatan. Kärnborning och installation av MLS*. S. E. AB.

Sweco. (2022a). *Blekingegatan Helsingborg. Uppdaterade platsspecifika riktvärden*. S. S. AB.

Sweco. (2022b). *Blekingegatan. Resultat från grundvattenprovtagning vid f.d. kemtvätt på Blekingegatan i Helsingborg*. S. S. AB.

Sweco. (2022c). *PM Rekommendationer rörande åtgärdsmetoder, Blekingegatan i Helsnigborg*. S. S. AB.

Sweco. (2023). *Blekingegatan. Grundvatttenprovtagning 2023 vid f.d kemtvätt på blekingegatan i Helsingborg.* S. S. AB.

Wanner, P. (2023). *PhD Course NGE006F. Stable isotope applications to assess chlorinated hydrocarbon (bio)degerdation [PowerPoint presentation]*. University of Gothenburg.

Wanner, P., Parker, B. L., Chapman, S. W., Aravena, R., & Hunkeler, D. (2016). Quantification of Degradation of Chlorinated Hydrocarbons in Saturated Low Permeability Sediments Using Compound-Specific Isotope Analysis. *Environmental Science & Technology*, *50*(11), 5622-5630. https://doi.org/10.1021/acs.est.5b06330

WHO. (2020). *Tetrachloroethene in drinking-water. Background document for development of WHO Guidelines for drinking-water*. (WHO/HEP/ECH/WSH/2020.9). License: CC BY-NC-SA 3.0 IGO). W. H. O. 2020.

Wiedemeier, T., Wilson, J., Hansen, J., Chapelle, F., & Swanson, M. (1996). Technical Protocol for Evaluating Natural Attenuation of Chlorinated Solvents in Groundwater. Revision 1. *The U.S. Environmental Protection Agency*(EPA/600/R-98/128 (NTIS 99-130023), 1998), 396.

WSP. (2015). *HUVUDSTUDIERAPPORT. Räven fd kemtvätt på blekingegatan, Helsingborg*. W. Environmental.

8 Appendices

Appendix A: Raw data

***Table A1**. Results of concentration analyses and measured field parameters from groundwater sampling March 2023.*

ELEMENT	SAMPLE	DFN3,1	DFN3,2	DFN3,3	DFN3,4	DFN3,5	DFN3,6	DFN5,1	DFN5,2	DFN5,3	DFN5,4	DFN5,5	DFN6,1	DFN6,2	DFN6,3	DFN6,4	DFN6,5	DFN 8:2	DFN 8:3	DFN 8:4	DFN 8:5	DFN 9:3	DFN 9:4	DFN 9:5	DFN 11:2	DFN 11:3	DFN 11:4	DFN 11:5	DFN 12:4	DFN 12,6	DFN13,5	DFN13,7	DFN 15:5	DFN 15:6	DFN 15:7	
Sampling Date		2023-03-21	2023-03-21	2023-03-21	2023-03-21	2023-03-21	2023-03-21	2023-03-21	2023-03-21	2023-03-21	2023-03-21	2023-03-21	2023-03-21	2023-03-21	2023-03-21	2023-03-21	2023-03-21	2023-03-23	2023-03-23	2023-03-23	2023-03-23	2023-03-23	2023-03-23	2023-03-23	2023-03-23	2023-03-23	2023-03-23	2023-03-23	2023-03-23	2023-03-23	2023-03-23	2023-03-21	2023-03-21	2023-03-23	2023-03-23	2023-03-23	
Filtrering		Nej	Nej	Nej	Nej	Nej	Nej	Ja	Nej	Nej	Nej	Nej	Nej	Nej	Nej	Nej	Nej	Ja	Ja	Ja	Ja	Ja	Ja	Ja	Ja	Ja	Ja	Ja	Ja	Ja	Nej	Ja	Ja	Ja	Ja	
bromid	mg/L	0,5	0,5	0,5	0,5	0,5	0,5	0,5	0,5	0,5	0,5	0,5	0,5	0,5	0,5	0,5	0,5	0,5	0,5	0,5	0,5	0,5	0,5	0,5	0,5	0,5	0,5	0,5	0,5	0,5	0,5	0,5	0,5	0,5	0,5	
Fe 2+ FÄLT	mg/L	10	3	0	0	10	0	25	0	3	0	3	0	10	10	10	0	0	0	0	3	0	0	0	0	0	3	10	0	10	10	10	0	0	0	
Fe 2+	mg/L			0,57	0,26	5,6	2,6	15		3,2	0,37		0,1	8,7	5,6	4,4	0,47	0,1	0,1	0,1	3,9	2,7	0,1	7,6	0,1	0,1	2,2	11	0,1	5,9	6,4	6,4	4,9	3,4	2,4	
Mn 2+	mg/L			0,084	0,01	0,12	0,066	1,4		0,29	0,034		0,01	4,2	0,33	0,44	0,022	0,044	0,22	2,6	1,4	0,29	0,85	0,52	0,032	1,1	3,6	2,2	0,19	2,8	0,33	0,31	0,46	0,3	0,31	
Ca, kalcium	mg/L	114	88,5	62	35,5	118	8,4	52,4	125	55,9	44,4	125	25,2	38,1	82,6	66,9	71,2	26,6	20,3	27,7	36,9	8,02	23,3	19,2	26,8	27,6	45	54,9	45,6	47,3	47,9	63,3	13,4	12,1	23,8	
K, kalium	mg/L	3,92	7,66	7,13	7,89	5,76	2,75	3,93	6,77	4,17	10,8	7,16	10,5	2,53	3,88	3,9	6,09	5,15	6,97	11,9	7,05	9,28	16,6	4,59	14,5	11,9	4,74	3,34	16,2	3,09	3,91	3,77	20,3	9,87	2,98	
Mg, magnesium	mg/L	6,58	19,6	14,5	9,67	12,6	1,73	7,96	17,4	4,99	12,8	15,4	4,57	11	5,95	5,61	13,8	10,1	6,8	9,65	7,87	2,88	7,76	3,02	6,18	7,19	14,8	9,09	11	13,1	15,6	5,86	1,78	4,13	2,38	
Na, natrium	mg/L	79,6	3,98	26,4	99,2	56,7	197	97,4	45,1	228	103	51,7	47,4	92,9	99,3	122	25	68,2	112	86,6	106	309	233	282	98,2	129	59,2	81,3	19,8	84,2	50,9	88,7	438	350	312	
tetrakloreten, PCE	µg/L	1,97	454	0,456	0,232	7,67	0,568	1160	848	36	19,2	46,9	678	6,61	134	616	0,18	8720	14900	27700	6730	35500	14600	815	2560	1450	220	135	10000	65,5	59,2	10,3	2010	258	169	
trikloreten, TCE	µg/L	42,4	554	5,28	4,43	15,2	5,71	408	358	5,63	11,4	26,5	53,4	942	272	825	0,12	1100	3840	5160	2560	13500	6560	1020	607	929	331	20,3	2680	59,7	368	23,5	3080	626	220	
cis-1,2-dikloreten, cDCE	µg/L	14,5	152	0,635	0,621	4,78	1,59	389	9,75	1	1,49	5,53	0,618	76,9	43,9	102	0,143	695	1560	1740	1280	1670	1130	1170	60,7	73,1	18,9	4,05	1040	49	32	8,39	502	84,8	27,1	
vinylklorid, VC	µg/L	1,21	4,7	0,1	0,1	0,1	0,1	1,12	1	1	0,1	0,1	0,1	6,64	2,97	4,95	0,1	1	1	1	2,69	1	1,13	1,86	1	1	1	1	1	1	1	1	2,41	1	1	
trans-1,2-dikloreten	µg/L	3,48	13,8	0,502	0,289	0,177	1,23	3,31	1	1	0,421	0,193	0,265	9,27	3,07	6,29	0,1	7,7	14,1	16,9	15,6	18,8	14,4	25,8	1,41	1,94	1	1	11,3	1,52	4,76	1	71,5	39,6	6,11	
1,1-dikloreten	µg/L	1,74	13,9	0,1	0,1	0,21	0,1	4,32	4,25	0,1	0,1	0,164	0,226	32,6	4,97	11,5	0,1	1,02	19,2	19,1	18,6	61,4	38,6	14,6	0,441	2,68	1,4	0,105	0,559	1,38	2,31	0,1	16,4	5,85	1,92	
1,1-dikloretan	µg/L	0,1	0,213	0,1	0,1	0,1	0,1	1	1	1	0,1	0,1	0,1	0,549	0,1	0,167	0,1	1	1	1	1	1	1	1	1	1	1	1	1	1	1	1	1	1	1	
1,2-dikloretan	µg/L	0,105	1,57	0,1	0,1	0,1	0,1	2,81	1	1	0,1	0,1	0,1	1,44	0,504	1,04	0,1	1	1	1,22	4,7	1	3,85	2,11	1	1	1,09	1	1	3,43	1,42	1	1,4	1,78	1	
1,1,1-trikloretan	µg/L	0,1	0,1	0,1	0,1	0,1	0,1	0,2	0,2	0,2	0,1	0,1	0,1	0,1	0,1	0,1	0,1	0,2	0,2	0,2	0,2	0,2	0,2	0,2	0,2	0,2	0,2	0,2	0,2	0,2	0,2	0,2	0,2	0,2	0,2	
1,1,2-trikloretan	µg/L	0,1	0,988	0,1	0,1	0,1	0,1	0,5	0,5	0,5	0,1	0,1	0,1	5,04	0,25	0,732	0,1	5,11	16,4	13,5	5,23	54,8	21,4	2,58	0,91	2,4	1,64	0,5	0,804	0,961	1,86	0,5	0,5	0,5	0,5	
tetraklormetan	µg/L	0,1	0,1	0,1	0,1	0,1	0,1	0,2	0,2	0,2	0,1	0,1	0,1	0,1	0,1	0,1	0,1	0,406	0,2	0,2	0,2	0,2	0,2	0,2	0,361	0,2	0,2	0,2	0,667	0,2	0,2	0,2	0,2	0,2	0,2	
diklormetan	µg/L	0,1	0,1	0,1	0,1	0,1	0,1	2	2	2	0,1	0,1	0,1	0,1	0,1	0,1	0,1	2	2	2	2	2	2	2	2	2	2	2	2	2	2	2	2	2	2	
1,2-diklorpropan	µg/L	0,1	0,1	0,1	0,1	0,1	0,1	1	1	1	0,1	0,1	0,1	0,1	0,1	0,1	0,1	1	1	1	1	1	1	1	1	1	1	1	1	1	1	1	1	1	1	
kloroform	µg/L	0,1	0,1	0,1	0,1	0,1	0,1	0,3	0,3	0,3	0,1	0,1	0,11	0,1	0,1	0,1	0,1	8,57	18,3	13,8	1,27	61,5	16,7	1,32	2,13	1,45	0,3	0,3	7,66	0,3	0,3	0,3	3,59	0,3	0,3	
DOC, löst organiskt kol	mg/L	4,47	11,2	6,27	4,78	5,03	1,8	3,15	4,1	7,04	3,34	5,81	3,01	2,87	4,3	5,5	4,73	4,1	5,04	4,13	5,76	14	10,9	10,6	4,03	4,16	3,06	3,45	3,31	2,81	1,98	3,56	13,4	8,75	11,4	
metan	µg/L	21,1	27,9	4070	1050	76,2	2620	87,9	2300	24,6	795	43,9	2	10,1	34,6	32,8	4760	2	2	2	8,2	2	2,4	5,3	2	2	2	3	2	2	2	7	2	2	8,6	
etan	µg/L	1	1	1	1	1	2,4	1,3	1	1	1	1	1	1	1	1	1	1	1	1	1	1	1	1	1	1	1	1	1	1	1	1	1	1	1	
eten	µg/L	1	1	1	1	1	1	1,5	1	1	1	1	1	1	1	1	1	1	1	1	1	1	1	1,5	1	1	1	1	1	1	1	1	1,9	1	1	
klorid	mg/L	52,1	68,8	20,5	33,3	56,1	15,5	67,8	80,6	110	46,9	57,5	17,7	52,7	56,5	57,6	29	55,2	46	32,1	46,5	39,7	32,6	56,3	17,9	26,5	44,1	71,7	23,8	68,6	50,4	89,8	24,3	49,9	71,5	
fluorid	mg/L	0,2	0,262	0,316	0,359	0,335	2,6	0,306	0,437	0,2	0,354	0,306	0,2	0,304	0,2	0,2	0,524	0,2	0,294	0,29	0,298	0,81	0,7	0,426	0,494	0,507	0,282	0,2	0,2	0,28	0,2	0,2	0,93	0,266	0,474	
nitrat, NO3	mg/L	2	2	2	2	2	2	2	2	2	2	2	55,8	2	2	2	2	44,3	32,9	12,2	2	28,2	5,28	2	65,8	25,7	2	2	28,3	2	2	2	2	2	2	
nitratkväve, NO3-N	mg/L	0,5	0,5	0,5	0,5	0,5	0,5	0,5	0,5	0,5	0,5	0,5	12,6	0,5	0,5	0,5	0,5	10	7,44	2,76	0,5	6,38	1,19	0,5	14,9	5,81	0,5	0,5	6,4	0,5	0,5	0,5	0,5	0,5	0,5	
sulfat, SO4	mg/L	81,2	72,4	8,2	48,7	111	5	42,1	7,92	111	32,2	111	36,3	55,4	64	63,4	5	36,5	42,7	48,8	49,5	55,9	68,7	58,6	34,9	45,5	67,6	59,6	47,6	54,6	62,9	56,3	50	77,2	69	
alkanintet	mg HCO3-/L	412	586	266	297	340	497	288	448	320	370	349	107	281	373	371	316	131	231	246	304	676	573	627	240	333	223	240	136	249	213	232	1090	817	681	
Provpunkt		DFN3,1	DFN3,2	DFN3,3	DFN3,4	DFN3,5	DFN3,6	DFN5,1	DFN5,2	DFN5,3	DFN5,4	DFN5,5	DFN6,1	DFN6,2	DFN6,3	DFN6,4	DFN6,5	DFN8,2	DFN8,3	DFN8,4	DFN8,5	DFN9,3	DFN9,4	DFN9,5	DFN11,2	DFN11,3	DFN11,4	DFN11,5	DFN12,4	DFN12,6	DFN13,5	DFN13,7	DFN15,5	DFN15,6	DFN15,7	
Provtagnings-datum		2023-03-20	2023-03-20	2023-03-20	2023-03-20	2023-03-20	2023-03-20	2023-03-21	2023-03-21	2023-03-21	2023-03-21	2023-03-21	2023-03-20	2023-03-20	2023-03-20	2023-03-20	2023-03-20	2023-03-23	2023-03-23	2023-03-23	2023-03-23	2023-03-22	2023-03-21	2023-03-21	2023-03-23	2023-03-22	2023-03-22	2023-03-22	2023-03-23	2023-03-23	2023-03-21	2023-03-21	2023-03-22	2023-03-22	2023-03-22	
Provtagnings-metod		Peristaltisk	Peristaltisk	Peristaltisk	Peristaltisk	Skakpump	DVP	DVP	DVP	DVP	DVP	DVP	Peristaltisk	Peristaltisk	Peristaltisk	Peristaltisk	Peristaltisk	Skakpump	ladderpump	DVP	DVP	DVP	DVP	DVP	DVP	DVP	DVP	Skakpump	Skakpump	Skakpump	Skakpump	Skakpump	Skakpump	Skakpump	
konduktivitet	mS/m	94,6	124,5	58,6	68	90,9	81,2	78,2	92,9	104,2	75,5	92,2	41,6	72,1	88,5	89,1	57,6	56,2	66,6	62,7	72,6	133,5	111,1	128,8	63,4	73,1	62,8	74,1	46,7	73,4	62,9	78,6	174	150	147,9	
pH		6,81	6,97	7,23	7,57	7,01	8,85	6,98	7,09	6,74	7,52	6,98	6,16	6,57	6,72	6,69	7,39	6,32	6,61	6,57	6,74	7,07	7,06	7,53	6,79	6,83	6,38	6,67	6,38	6,54	6,35	6,62	8,43	7,84	7,72	
redox	mV	-117,1	-111	-120,5	-113,8	-130,1	-153,7	-119	-78	-72	-97	-73	48,3	-100,1	-107,8	-111,4	-168,7	79	42,2	29,5	-88,5	17,3	-38	-125	107,8	-18	-58	-104	68,4	-67,2	-14	-49	49	-43	-43	
syre	%	-0,7	-1,2	0,2	-0,3	-0,2	1,8	2,8	8,6	6,9	18,1	12,2	39,8	-1,7	-2,3	-1,8	-1,4	17	20,5	3,4	5	5	7,8	4,6	16	3	0,4	1,9	4	1,2	10,9	21,7	13,2	21,1	10,1	
syre	mg/L	-0,08	-0,14	0,02	-0,03	-0,03	0,2	0,31	0,97	0,78	2,06	1,37	4,38	-0,19	-0,25	-0,2	-0,16	1,99	2,37	0,37	0,55	0,55	0,88	0,51	1,84	0,34	0,05	0,22	0,43	0,13	1,22	2,54	1,49	2,44	1,16	
temperatur	°C	11,1	11,2	11	10,8	10,5	10,2	10,8	10	9,3	9,6	10	11	10,8	11,3	11,4	1,3	8,6	8,8	11,3	10,5	11	10,1	10,5	9,2	10	10,4	10	11,8	12,2	9,2	8,3	9,4	8,6	8,8	
		DFN3						DFN5					DFN6					DFN8				DFN9			DFN11				DFN12		DFN13		DFN15			Källområde Medelvärde
Redox Medelvärde	mV	-124,36667						-87,8					-87,94					15,55				-48,566667			-18,05				0,6		-31,5		-12,333333			-30,15217391
Metan medelvärde	µg/L	1310,8667						650,28					967,9					3,55				3,2333333			2,25				2		4,5		4,2			143,9086957

***Table A2**. Results of conducted CSIA of groundwater samples collected March 2023*

Sample	cDCE d13C	Average	STDEV	STE	∂% from STD	TCE d13C	Average	STDEV	STE		PCE d13C	Average	STDEV	STE
SGU_DFN3_2_1	-23,51					-26,91					-20,26			
SGU_DFN3_2_2	-24,77					-27,05					-19,64			
SGU_DFN3_2_3	-24,38	**-24,22**	**0,64**	**0,37**		-27,23					-19,87			
SGU_DFN3_2_4						-27,19	**-27,09**	**0,15**	**0,08**		-19,98	**-19,94**	**0,25**	**0,15**
SGU_DFN5_1_1						-23,70					-24,48			
SGU_DFN5_1_2						-23,24					-24,50			
SGU_DFN5_1_3						-22,98	**-23,31**	**0,36**	**0,21**		-24,17	**-24,38**	**0,19**	**0,11**
SGU_DFN5_2_1						-23,41					-22,68			
SGU_DFN5_2_2						-23,20					-22,47			
SGU_DFN5_2_3						-23,24	**-23,28**	**0,12**	**0,07**		-22,47	**-22,54**	**0,12**	**0,07**
SGU_DFN6_1_1											-23,53			
SGU_DFN6_1_2											-23,42			
SGU_DFN6_1_3											-23,43	**-23,46**	**0,06**	**0,03**
SGU_DFN6_2_1						-20,53								
SGU_DFN6_2_2						-21,02								
SGU_DFN6_2_3						-21,42	**-21,22**	**0,29**	**0,16**					
SGU_DFN6_3_1						-24,12					-20,27			
SGU_DFN6_3_2	-22,08					-23,77					-20,55			
SGU_DFN6_3_3	-22,74	**-22,41**	**0,47**	**0,27**		-24,11	**-24,00**	**0,20**	**0,11**		-20,66	**-20,49**	**0,20**	**0,12**
SGU_DFN6_4_1	-23,73					-24,89					-20,52			
SGU_DFN6_4_2	-23,28					-24,65					-20,13			
SGU_DFN6_4_3	-22,42	**-23,14**	**0,67**	**0,39**		-24,42	**-24,65**	**0,23**	**0,13**		-20,45	**-20,37**	**0,21**	**0,12**
SGU_DFN8_2_1	-24,93					-22,50					-25,73			
SGU_DFN8_2_2	-24,96					-22,16					-25,49			
SGU_DFN8_2_3	-24,81	**-24,90**	**0,08**	**0,05**		-22,19	**-22,28**	**0,19**	**0,11**		-25,61	**-25,61**	**0,12**	**0,07**
SGU_DFN8_3_1	-24,11					-22,65					-25,85			
SGU_DFN8_3_2	-24,71					-22,39					-25,61			
SGU_DFN8_3_3	-24,41	**-24,41**	**0,30**	**0,17**		-22,57	**-22,54**	**0,13**	**0,08**		-25,73	**-25,73**	**0,12**	**0,07**
SGU_DFN8_4_1	-24,44					-22,31					-25,61			
SGU_DFN8_4_2	-24,54					-22,57					-25,30			
SGU_DFN8_4_3	-24,29	**-24,42**	**0,12**	**0,07**		-22,31	**-22,40**	**0,15**	**0,09**		-25,33	**-25,41**	**0,17**	**0,10**
SGU_DFN8_5_1	-24,36					-23,77					-24,92			
SGU_DFN8_5_2	-24,19					-23,98					-24,51			
SGU_DFN8_5_3	-24,29	**-24,28**	**0,09**	**0,05**		-23,81	**-23,86**	**0,11**	**0,06**		-24,58	**-24,67**	**0,22**	**0,13**
SGU_DFN9_3_1	-24,44					-22,13					-22,67			
SGU_DFN9_3_2	-24,29					-22,21								
SGU_DFN9_3_3	-24,25	**-24,32**	**0,10**	**0,06**		-21,76	**-22,03**	**0,24**	**0,14**		-22,98	**-22,82**	**0,22**	**0,12**
SGU_DFN9_4_1	-23,77					-22,28					-23,36			
SGU_DFN9_4_2						-22,47					-23,17			
SGU_DFN9_4_3	-23,74	**-23,76**	**0,03**	**0,01**		-22,22	**-22,33**	**0,13**	**0,08**		-23,73	**-23,42**	**0,29**	**0,17**
SGU_DFN9_5_1	-24,56					-23,96					-23,48			
SGU_DFN9_5_2	-24,55					-24,18					-23,33			
SGU_DFN9_5_3	-24,29	**-24,47**	**0,15**	**0,09**		-24,20	**-24,11**	**0,13**	**0,08**		-23,37	**-23,39**	**0,08**	**0,05**
SGU_DFN11_2_1						-21,59					-23,42			
SGU_DFN11_2_2	-22,25					-21,61					-23,39			
SGU_DFN11_2_3	-23,08	**-22,66**	**0,59**	**0,34**		-21,56	**-21,59**	**0,03**	**0,02**		-22,84	**-23,22**	**0,33**	**0,19**
SGU_DFN11_3_1						-20,75					-23,19			
SGU_DFN11_3_2						-20,67					-23,05			
SGU_DFN11_3_3						-20,70	**-20,71**	**0,04**	**0,02**		-23,03	**-23,09**	**0,09**	**0,05**
SGU_DFN11_4_1						-17,57					-22,80			
SGU_DFN11_4_2						-20,32					-22,34			
SGU_DFN11_4_3						-20,14	**-20,23**	**0,13**	**0,09**		-22,60	**-22,58**	**0,23**	**0,13**
SGU_DFN11_5_1						-18,31					-23,81			
SGU_DFN11_5_2						-20,15					-22,98			
SGU_DFN11_5_3						-19,11	**-19,19**	**0,92**	**0,53**		-23,03	**-23,01**	**0,04**	**0,03**
SGU_DFN12_4_1	-22,76					-21,83					-23,90			
SGU_DFN12_4_2						-21,58					-24,18			
SGU_DFN12_4_3	-22,11	**-22,43**	**0,46**	**0,26**		-21,55	**-21,65**	**0,16**	**0,09**		-23,77	**-23,95**	**0,21**	**0,12**
SGU_DFN12_6_1	-21,56					-20,61					-24,15			
SGU_DFN12_6_2	-22,33					-19,18					-23,35			
SGU_DFN12_6_3	-21,09	**-21,66**	**0,63**	**0,36**		-20,31	**-20,04**	**0,75**	**0,43**		-24,20	**-23,90**	**0,47**	**0,27**
SGU_DFN13_5_1	-23,44					-20,19					-21,92			
SGU_DFN13_5_2	-21,87					-19,98					-23,05			
SGU_DFN13_5_3	-19,25	**-21,52**	**2,12**	**1,22**		-20,30	**-20,16**	**0,16**	**0,09**		-22,55	**-22,50**	**0,57**	**0,33**
SGU_DFN15_5_1						-21,03					-20,52			
SGU_DFN15_5_2						-21,52	**-21,28**	**0,34**	**0,24**		-20,87	**-20,69**	**0,25**	**0,17**
SGU_DFN15_5_3														
SGU_DFN15_6_1						-19,50					-20,50			
SGU_DFN15_6_2	-25,77					-20,00					-20,55			
SGU_DFN15_6_3	-25,68	**-25,72**	**0,07**	**0,05**		-19,15	**-19,55**	**0,43**	**0,25**		-20,51	**-20,52**	**0,03**	**0,01**
SGU_DFN15_7_1						-20,13					-22,32			
SGU_DFN15_7_2						-20,26								
SGU_DFN15_7_3						-18,81	**-19,73**	**0,80**	**0,46**		-21,85	**-22,09**	**0,33**	**0,19**
												Total Samples:	**24**	

Standard	cDCE d13C	Average	STDEV	TCE d13C	Average	STDEV	PCE d13C	Average	STDEV
SGU_STD_1	-25,06	-24,57	0,37	-24,25	-23,69	0,43	-27,23	-27,33	0,31
SGU_STD_2	-25,04			-24,23			-27,81		
SGU_STD_3	-25,00			-24,29			-27,51		
SGU_STD_4	-25,00			-24,29			-27,62		
SGU_STD_5	-24,65			-23,81			-27,38		
SGU_STD_7	-24,55			-23,51			-27,18		
SGU_STD_8	-24,21			-23,26					
SGU_STD_9	-24,47			-23,49			-26,91		
SGU_STD_10	-24,46			-23,46					
SGU_STD_11	-24,22			-23,38					
SGU_STD_12	-24,08			-23,29			-27,00		
SGU_STD_13	-24,05			-23,05					

***Table A3**. Results of chlorinated solvents concentration analysis of groundwater samples collected 2019. Highest concentration of PCE detected, highlighted in yellow.*

Provpunkt	*Provtagningsdatum*	tetrakloreten (µg/l)	trikloreten (µg/l)	cis-1,2-dikloreten (µg/l)	trans-1,2-dikloreten (µg/l)	vinylklorid (µg/l)
DFN3.1	*2019-11-06*	140	160	22	1,9	1,6
DFN3.2	*2019-11-06*	1500	1500	180	9,5	5,9
DFN3.3	*2019-11-06*	40	34	3,4	0,22	0,12
DFN3.4	*2019-11-06*	49	44	5,3	0,26	0,15
DFN3.5	*2019-11-06*	140	140	19	0,75	0,32
DFN3.6	*2019-11-06*	100	130	16	0,28	<0,1
DFN5.1	*2019-11-07*	1080	353	74,3	1,82	<10
DFN5.2	*2019-11-07*	924	117	7,21	<1	<10
DFN5.3	*2019-11-07*	70	9,72	0,34	<0,1	<1
DFN5.4	*2019-11-07*	270	71	9,8	0,21	<0,1
DFN5.5	*2019-11-07*	860	370	77	1,6	0,28
DFN4.8	*2019-11-26*	170	6,4	0,7	0,12	<0,1
DFN3.1	*2019-11-28*	30	100	17	1,8	1,9
DFN3.2	*2019-11-28*	1500	1700	170	9	5,5
DFN3.2.1	*2019-11-28*	1500	1700	170	8,9	5,3
DFN3.3	*2019-11-28*	17	18	2,1	0,13	<0,1
DFN3.4	*2019-11-28*	18	21	3,1	0,23	<0,1
DFN3.5	*2019-11-28*	120	130	16	0,81	0,66
DFN3.6	*2019-12-03*	77	78	9,9	0,51	0,34
DFN5.1	*2019-12-03*	9330	964	135	<10	<100
DFN5.2	*2019-12-03*	178000	4770	15	<10	<100
DFN5.3	*2019-12-03*	2,7	0,77	<0,1	<0,1	<1
DFN5.4	*2019-12-03*	54	16	2,5	<0,1	<0,1
DFN5.5	*2019-12-03*	450	150	28	0,67	0,13
DFN2.1	*2019-12-18*	0,021	<0,02	<0,02	<0,02	<0,02
DFN2.2	*2019-12-18*	0,028	<0,02	<0,02	<0,02	<0,02
DFN2.8	*2019-12-18*	<0,02	<0,02	<0,02	<0,02	<0,02
DFN4.1	*2019-12-18*	<0,02	<0,02	<0,02	<0,02	<0,02
DFN4.2	*2019-12-18*	0,077	<0,02	<0,02	<0,02	<0,02
DFN4.3	*2019-12-18*	0,081	0,022	<0,02	0,034	<0,02
DFN4.4	*2019-12-18*	<0,02	<0,02	<0,02	<0,02	<0,02
DFN4.5	*2019-12-18*	0,029	0,023	<0,02	<0,02	<0,02
DFN4.6	*2019-12-18*	0,026	<0,02	<0,02	<0,02	<0,02
DFN4.7	*2019-12-18*	<0,02	<0,02	<0,02	0,039	<0,02
DFN4.8	*2019-12-18*	120	2	0,37	0,064	<0,02
DFN1.1	*2019-12-19*	0,16	0,025	<0,02	<0,02	<0,02
DFN1.2	*2019-12-19*	0,47	0,091	<0,02	<0,02	<0,02
DFN1.3	*2019-12-19*	<0,02	<0,02	<0,02	<0,02	<0,02
DFN2.3	*2019-12-19*	<0,02	<0,02	<0,02	<0,02	<0,02
DFN2.4	*2019-12-19*	0,76	0,14	0,03	<0,02	<0,02
DFN2.5	*2019-12-19*	0,083	<0,02	<0,02	<0,02	<0,02
DFN2.6	*2019-12-19*	0,39	0,036	<0,02	<0,02	<0,02
DFN2.7	*2019-12-19*	<0,02	<0,02	<0,02	<0,02	<0,02
DFN3.1	*2019-12-19*	20	62	15	1,3	0,73
DFN3.2	*2019-12-19*	1400	990	170	15	9,8
DFN3.3	*2019-12-19*	29	24	2,4	0,2	0,13
DFN3.4	*2019-12-19*	8,7	6,6	1,1	0,055	0,049
DFN3.5	*2019-12-19*	15	20	4,3	0,15	<0,02
DFN3.6	*2019-12-19*	0,94	1,4	0,31	<0,02	<0,02
DFN5.1	*2019-12-20*	786	292	78,8	3,28	<1
DFN5.2	*2019-12-20*	13700	1000	<10	<10	<100
DFN5.3	*2019-12-20*	21,9	1,44	<0,1	<0,1	<1
DFN5.4	*2019-12-20*	47	20	3,2	0,1	<0,02
DFN5.5	*2019-12-20*	330	97	41	1,2	0,26

Appendix B: Profile diagrams of the source transect

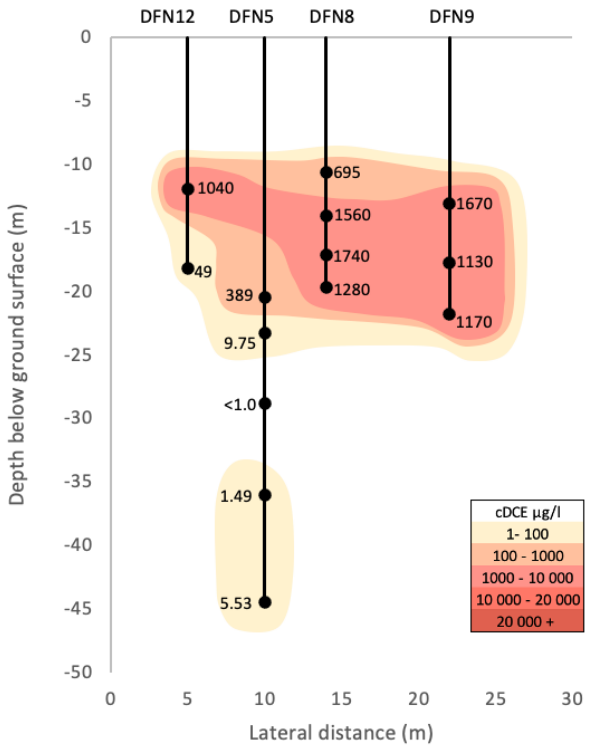

***Figure A1**. Concentration diagram of source transect with concentration data of cDCE in µg/l.*

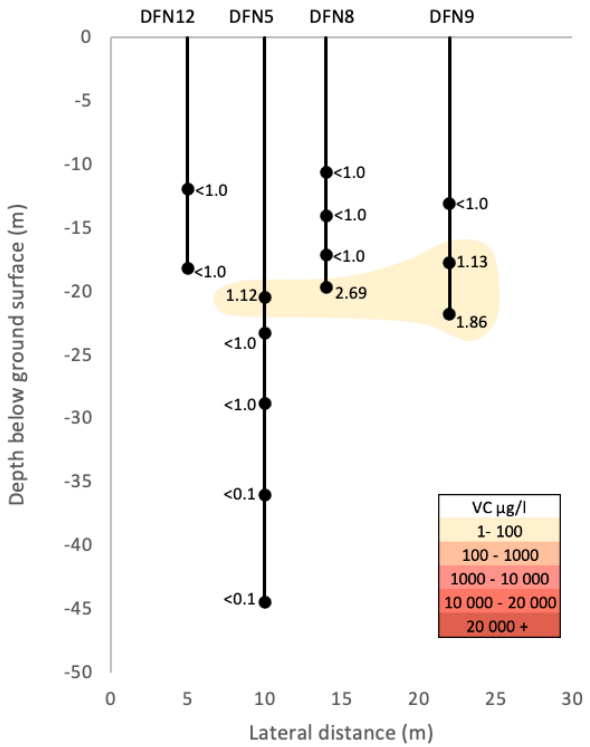

***Figure A2**. Concentration diagram of source transect with concentration data of VC in µg/l.*

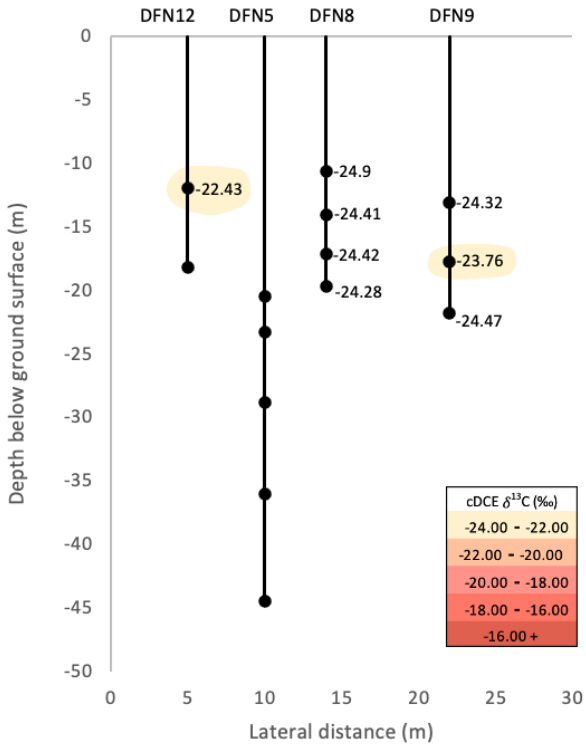

***Figure A3**. Diagram of source transect with $\delta^{13}C$ values of cDCE in permill (‰).*